

1 Competition between lysogenic and sensitive bacteria is determined
2 by the fitness costs of the different emerging phage-resistance
3 strategies

4
5 Olaya Rendueles*, Jorge A.M. de Sousa and Eduardo P.C. Rocha

6
7 ¹ Institut Pasteur, Université Paris Cité, CNRS UMR3525, Paris, 75015, France.

8 *corresponding author : olaya.rendueles-garcia@pasteur.fr
9

10 **ORCID:** OR, 0000-0002-6648-1594, JAMdS, 0000-0003-3530-8550; EPCR, 0000-0001-7704-822X.

11
12 **Keywords:** Interspecies competition

13
14 **Running title:** Emergence of resistance against *Klebsiella* phages
15
16
17

ABSTRACT

Many bacterial genomes carry prophages whose induction can eliminate competitors. In response, bacteria may become resistant by modifying surface receptors, by lysogenization, or by other poorly known processes. All these mechanisms affect bacterial fitness and population dynamics. To understand the evolution of phage resistance, we co-cultivated a phage-sensitive strain (BJ1) and a poly-lysogenic *Klebsiella pneumoniae* strain (ST14) under different phage pressures. The population yield remained stable after 30 days. Surprisingly, the initially sensitive strain remained in all populations and its frequency was highest when phage pressure was strongest. Resistance to phages in these populations emerged initially through mutations preventing capsule biosynthesis. Protection through lysogeny was rarely observed because the lysogens have increased death rates due to prophage induction. Unexpectedly, the adaptation process changed at longer time scales: the frequency of capsulated cells in BJ1 populations increased again, because the production of capsule was fine-tuned, reducing the ability of phage to absorb. Contrary to the lysogens, these capsulated resistant clones are pan-resistant to a large panel of phages. Intriguingly, some clones exhibited transient non-genetic resistance to phages, suggesting an important role of phenotypic resistance in coevolving populations. Our results show that interactions between lysogens and sensitive strains are shaped by antagonistic co-evolution between phages and bacteria. These processes may involve key physiological traits, such as the capsule, and depend on the time frame of the evolutionary process. At short time scales, simple and costly inactivating mutations are adaptive, but in the long-term, changes drawing more favorable trade-offs between resistance to phages and cell fitness become prevalent.

41

42 INTRODUCTION

43

44 Parasites shape the life history and fitness of their hosts. They also impact community
45 structure via predation and competition, and thereby affect numerous ecological and
46 evolutionary processes (1-3). Bacteriophages (phages) are very abundant predators of bacteria
47 (4, 5). Temperate phages either follow a lytic cycle in which they replicate within bacterial
48 cells and release infectious virions, or a lysogenic cycle in which they integrate the bacterial
49 genome and replicate with it. Nearly half of the sequenced bacterial genomes are lysogens (6).
50 The dual lifestyle of temperate phages is costly, but can also provide the host with multiple
51 advantages. During lysogeny, prophages may increase biofilm formation (7), phosphate
52 acquisition (8), or express virulence factors (9-11). Inactivated prophages leave genes in the
53 genome that are co-opted by the host and result in functional innovation, e.g. as bacteriocins
54 used in bacterial warfare (12-14). Prophages also protect bacteria from closely related phages,
55 a process called superinfection resistance (15). Furthermore, when the lytic cycle is initiated
56 in a small subpopulation, it may facilitate colonization by directly mediating competition
57 within communities (16-19), because the released virions will infect and lyse closely-related
58 but not identical strains. This can promote the acquisition of adaptive traits from bacterial
59 competitors (19, 20). Hence, it is suggested that prophage induction affects bacterial
60 population dynamics, community structure, and evolution (21-25).

61 How parasite pressure may alter co-evolving bacterial populations has been seldom
62 addressed, and most of these studies focused on virulent phages (26-30). A few other studies
63 have tested the impact of coevolution between lysogens and non-lysogens and the advantages
64 the former provide *in vivo* by mediating bacterial interactions (17, 23, 31-33). However, the
65 relevance of poly-lysogeny for population dynamics during hundreds of generations remains
66 unknown. Further, little is known about the interactions between the different resistance
67 mechanisms, how they affect the cost of resistance, and how they may provide opportunity
68 for the emergence of novel mechanisms. To test this, we co-evolved two natural isolates of
69 *Klebsiella pneumoniae*, an ubiquitous species, of which at least 75% of the species' genomes
70 are polylysogenic (34): i) the hypervirulent BJ1 strain without inducible or cryptic prophages,
71 that was isolated from a liver abscess (ST380) and ii) a polylysogenic multidrug resistant *K.*
72 *pneumoniae* strain (ST14) isolated from a urinary tract nosocomial infection. ST14 produces
73 multiple infectious virions for which the BJ1 is known to be sensitive (Supplementary File 1)

(34). Based on previous studies, cell defence mechanisms, such as restriction modification systems, are not expected to impact population dynamics (34). We hypothesized that resistance would rather emerge by lysogenization under strong phage pressure and by inactivation of the extracellular capsule, the main surface receptor of phage at intermediate and low phage pressure (34). To test if, and how, prophage induction affects the competition outcome between the two strains, we followed their population dynamics through time. We then tested for the emergence of phage resistance in the susceptible strain. This revealed the diversity and interactions of the emerging mechanisms of phage resistance. It also provided unique insight into how these different mechanisms coexist within a population and evolve through time in response to infection pressure.

RESULTS

Temperate phages provide fitness advantage during competition

We first aimed at understanding if the prophages of strain ST14 provide a fitness advantage during competition with phage susceptible strain BJ1. To limit confounding factors such as competition for resources, we grew the cells in a rich environment. To modulate the amount of phage produced, and the ability of the latter to infect, we defined three conditions: (i) LB, (ii) LB supplemented with 0.2% citrate to inhibit phage infection due to calcium chelation (34, 35) and (iii) LB with mytomicin C (MMC, 0.1 µg/mL) to increase the phage titers in the environment. MMC was added at a concentration that did not significantly affect growth of BJ1 (Figure 1 – Figure Supplement 1AB), and despite the consumption of citrate by *Klebsiella*, after 24 hours there is still a large amount of citrate remaining, that is sufficient to inhibit infection (Figure 1 – Figure Supplement 1). We also quantified the amount of PFU/mL produced by strain ST14 in the different growth conditions. As expected, phage production in ST14 was significantly higher in MMC compared to the two other treatments. Interestingly, ST14 grown in citrate resulted in a marginal increase phage production relative to the control (LB) (Figure 1 – Figure Supplement 1CD).

To test whether phages could contribute to the competitive fitness of their host, we co-inoculated both strains (BJ1 and ST14) at an initial ratio of 1:1 for 24 hours. First, we tested if mixing the two strains affected the total growth or the population yield. We observed no increased cell death due to the competition in the different growth conditions (Figure 1 – Figure Supplement 2A). Then, we calculated the competitive index of the strains and observed that there was a large fitness advantage for strain ST14 in all three conditions

(Figure 1A). This was most likely because ST14 has both a higher growth rate and population yield than BJ1, except in the presence of MMC (Figure 1 – Figure Supplement 1AB). Most importantly, we also observed differences in the competitive index depending on the amount of phage released, or its ability to infect the BJ1 (Kruskal-Wallis, $dF=2$, $P=0.006$). This effect could be due to the different population yields of each strain in each environment (Figure 1 – Figure Supplement 2B). To take into account only the fitness effects due to phages, we quantified the strain-interaction effects using $C_i(j)$, which measures the effect of mixing two strains i and j on the viable population size of strain i , relative to pure culture controls. This measure accounts for the absolute performance of each competitor in mixed groups (see Methods). Negative $C_i(j)$ values indicate that strain i have lower population yield during growth in the presence of j than in pure culture, and positive values indicate the opposite. For the phage producer, strain ST14, the competition had no positive or negative effect on total population yield, most likely because increased release of viruses resulting in ST14 death is outweighed by an exacerbated death of phage-sensitive BJ1 (Figure 1B). In the presence of citrate, a condition in which phage cannot infect, the growth of strain BJ1 was not significantly inhibited. However, in the absence of citrate, when phages can infect, $C_i(j)$ was significantly lower than zero, indicating a negative effect on the growth of strain BJ1. This effect was dependent on the amount of phage released into the environment, as an increased production of phages by ST14 due to MMC leads to an even lower $C_i(j)$ for BJ1 (Figure 1B, Kruskal-Wallis, $dF=2$, $P=0.007$).

We also tested whether ST14 could sense the presence of competition, for instance by quorum sensing mechanisms, and induce prophages and the production viral particles (36). Our results showed that growth of ST14 with spent supernatant of BJ1 did not result in increased viral release (Figure 1 – Figure Supplement 1CDE). Taken together, our results showed that prophages can increase fitness of their host in co-culture by disfavouring the non-lysogens.

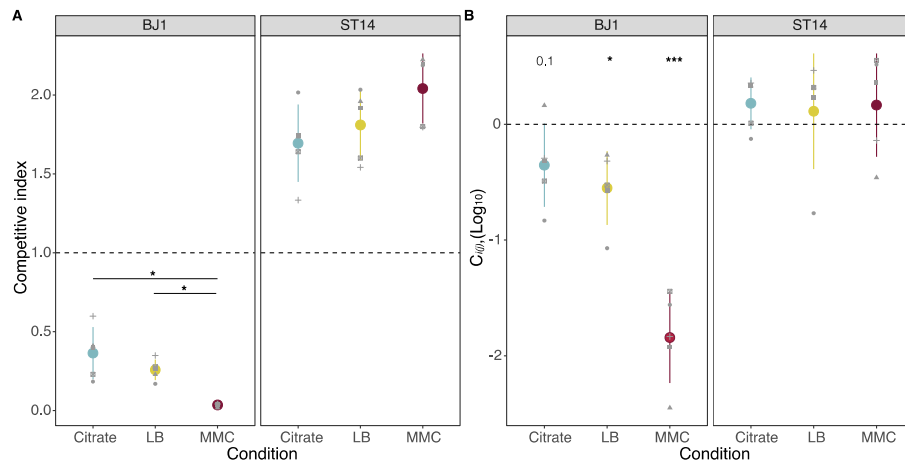


Figure 1. Fitness of strains during competition. **A.** The competitive index is calculated as the final frequency of each strain divided by the initial frequency in the mixed cocultures. * $P < 0.05$, Wilcoxon rank sum test adjusted by Benjamini-Hochberg correction. **B.** The effect of mixing two strains during growth in coculture is given as C_{ij} , expressed in \log_{10} , with i representing either strain BJ1 or strain ST14. Positive values represent increased cell numbers during coculture than those expected from the pure cultures. P values corresponds to one-sample t-test for difference of 0. * $P < 0.05$, *** $P < 0.001$. Each dot shape represents an independent biological replicate, $N=5$. Error bars indicate the standard deviation.

Resistance to temperate phages emerges rapidly during coevolution

To assess whether ST14 prophages could provide a long-term fitness advantage to their hosts, and allow them to outcompete non-lysogens, we set up an experiment in which we allowed three independent mixed populations composed of phage-producing ST14 and phage-susceptible BJ1 strains to coevolve during 30 days, in the three previously defined environments (LB, LB supplemented with 0.2% citrate and LB supplemented with MMC). To follow the evolution of each strain, we plated the populations every day on selective media and counted CFU. As expected, no significant changes in the group yield were observed (Figure 2 – Figure Supplement 1). This is mostly explained because the dominant strain, the phage producer, does not change its population yield (Figure 2A). In contrast, the frequency of BJ1 decreased rapidly during the first 4 days, suggesting a large initial fitness disadvantage of this strain. This is observed in all three conditions, but it is accelerated in conditions in which phage release is exacerbated (with MMC) and bacterial infection is not restricted (without citrate). Decrease of BJ1 populations also correlated with large increases in phage production during the first ten days (Figure 2 – Figure Supplement 2). Interestingly, shortly after the beginning of the experiment, both phage production and evolved BJ1 populations seem to stabilize, except for one BJ1 population evolving in MMC (which increases significantly in frequency). This suggested the emergence of phage resistance. However, after day 15, BJ1 populations evolving in MMC remain stable whereas the ones in the other conditions showed a second decrease in CFUs. This second decrease continued until day 22,

beyond which BJ1 populations once again stabilized at *ca* 10³ CFU/mL. Taken together, in 30 days of coevolution, ST14 did not completely displace BJ1 from the populations, even in conditions where the production of the phage by strain ST14 is exacerbated. Indeed, across all conditions, and throughout all the experimental evolution, infectious virions were actively produced and released (Figure 2 – Figure Supplement 2), representing a constant, active selective pressure. This suggests that prophage-mediated competition can be counter-balanced by the evolution of resistance mechanisms in the competitor strain.

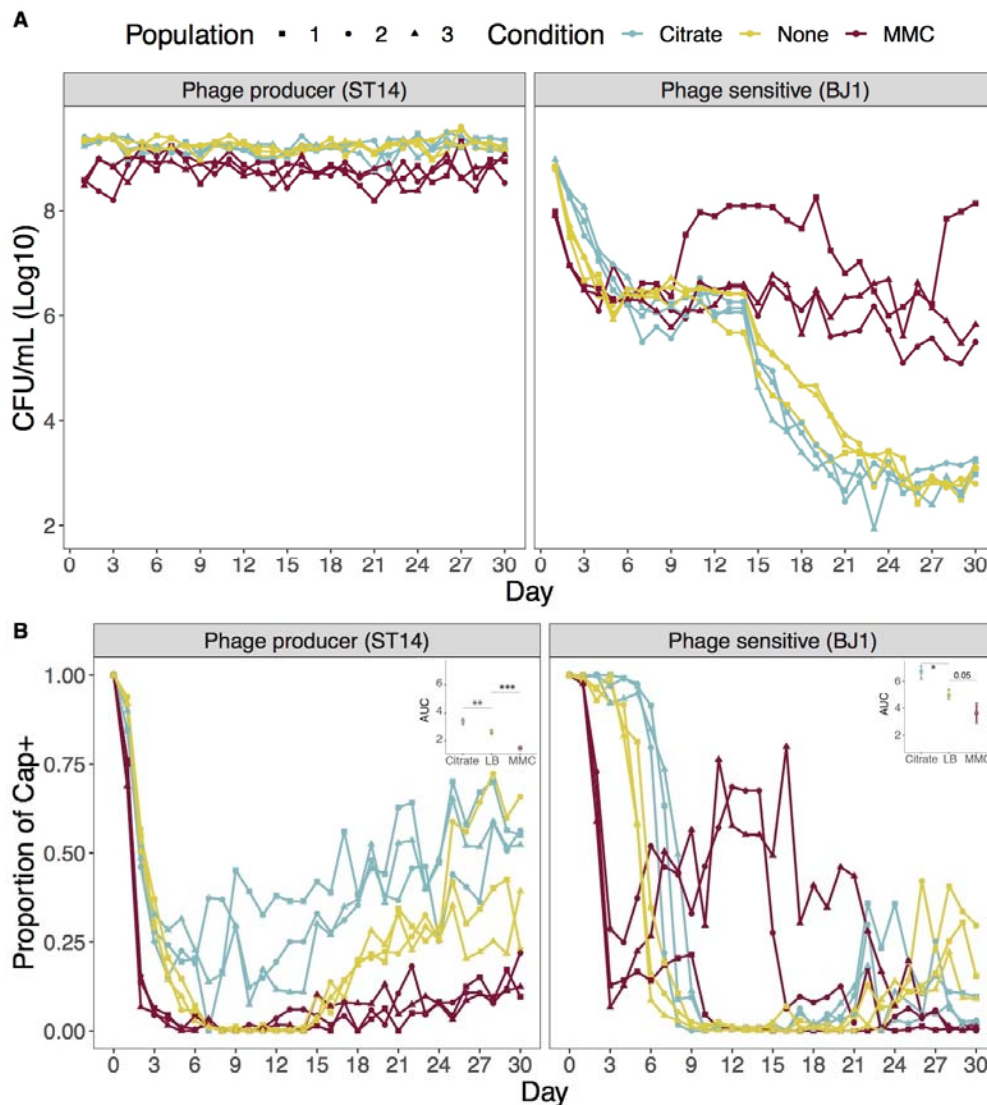


Figure 2. Population yield and proportion of capsulated clones of the two strains during the coevolution experiment. **A.** Total CFU per mL of each strain as estimated every day on selective media. Each line represents an independent coevolving population. **B.** Emergence of non-capsulated mutants in each strain. The proportion of capsulated clones in the population is depicted. The insert shows the area under the curve (AUC) during the first 9 days of evolution, as calculated by the function *trapz* from the R package *pracma*. * $P < 0.05$, ** $P < 0.01$, *** $P < 0.001$ for ANOVA with Tukey *post hoc* corrections.

Phage pressure drives receptor inactivation as a mechanism of resistance

It has been largely documented that the extracellular capsule is a main phage receptor in *Klebsiella* (34, 37-39). Throughout the daily plating of coevolving populations, we observed the rapid emergence of non-capsulated clones in all independent populations across the three treatments (Figure 2B). We tested if non-capsulated clones could be under stronger selection for receptor inactivation when phage pressure is higher (higher density of phages). We observed that the emergence of non-capsulated clones in the BJ1 background is exacerbated in the environment in which phage pressure is greater (insert, Figure 2B), and is diminished when phages cannot infect. Hence, phage pressure accelerated capsule inactivation. Interestingly, this is also the case for ST14, the phage producer, which we had previously shown to be mildly susceptible to its own phages (34). Overall, within the first ten days, at least 50% of the population was composed of non-capsulated mutants. Towards the end of the experiment, increasing frequencies of capsulated clones were observed across many populations, suggestive of the emergence of other resistance mechanisms. We sequenced the gene *wcaJ* to identify the genetic causes of receptor inactivation because it encodes the first glycosyltransferase of the capsule biosynthesis pathway and is known to be largely responsible for capsule inactivation (40, 41). This revealed that all but two non-capsulated clones (BJ1 (N=36); ST14 (N = 18)) had mutations in *wcaJ*, most of which resulted in a loss-of-function (Supplementary File S2). In summary, phage pressure led to rapid resistance emergence by surface modifications.

The emergence of new lysogens is rare and potentially unstable

Some resistant clones of strain BJ1 are capsulated, which lead us to hypothesize that they evolved other resistance mechanisms. To test this, we analysed at different time points the resistance mechanisms of the capsulated clones in the population. We expected to find BJ1 lysogens, since super-infection exclusion due to the lysogenization of capsulated bacteria could prevent further infection by the same phages. Further, our previous work had already shown that, when infected with phage lysate at high titers, at least two of the four intact phages from strain ST14 could lysogenize BJ1 (Supplementary File 1) (34). To quantify the proportion of lysogenized BJ1 cells, relative to other resistance mechanisms, we isolated over 1200 capsulated clones at different time points (Figure 3 – Figure Supplement 1). We identified the clones that were resistant to purified phage lysates of strain ST14 and that produced phages when exposed to MMC in our culture conditions. More precisely, we

analysed the differences in the area under the growth curve of each clone, both when they were grown in LB (control), when phage lysate was added (to distinguish between resistant or susceptible), and when MMC was added (to induce prophages and identify newly lysogenic clones). Together with the resistant non-capsulated clones (Figure 2B), this provides a detailed overview of the different mechanisms of resistance, their proportion, and their temporal dynamics throughout the experiment (Figure 3).

We first observed that the proportion of susceptible clones quickly decreased, especially when phage pressure was high (under MMC, Figure 3). The majority of tested clones were resistant by day 2, 6 and 8 in populations evolving in MMC, LB and citrate, respectively. As expected, lysogens emerged in all populations, but remained at low frequency and their numbers quickly dwindled after their emergence (Figure 3). We verified that the 94 identified lysogens, out of the 1209 screened clones, were *bona fide* lysogens. This could be confirmed by their production of phages infecting naïve BJ1 cells, both when induced by MMC (92 out of 94), and in the absence of induction (87 clones out of 94) (Figure 3 – Figure Supplement 2).

Interestingly, we observed that when new lysogens are grown in LB, in the absence of induction, there is a detectable amount of cell death, and growth delay at the end of exponential phase in at least in 29 out of 94 tested clones (Figure 3B and Figure 3 – Figure Supplement 4). This could correspond to a high frequency of spontaneous induction in the newly lysogenized bacteria. Indeed, we observed a large amount of phage release, as evidenced by large inhibition halos on an overlay of ancestral BJ1. We then selected five different lysogens that consistently showed large inhibition halos (Figure 3 – Figure Supplement 2) and exacerbated death (Figure 3B and S7) descending from three independently evolving BJ1 populations. We quantified the amount of phage released, in the absence of induction, on a lawn of ancestral BJ1. New lysogens produced between 100 and 1000 more PFU/mL than the ancestral phage producer (ST14) (Figure 3C). This suggests that protection by lysogeny results in significant fitness costs because prophage induction is frequent (Figure 3 – Figure Supplement 2 and 3A).

To study the impact of prophage acquisition in the long-term stability of lysogens in a population, we used eVIVALDI, an individual-based model for microbial interactions and evolution (42). We used these simulations to explore different rates of induction of prophages, in the presence or absence of abiotic agents. We designed a scenario where a population of initially sensitive bacterial cells is exposed to an inoculum of temperate phages, and we

249 followed the populations for a period of 150 iterations (e.g., approximately 150 generations).
250 Simulated bacteria could either be infected by phage (thus either dying upon a lytic infection
251 or becoming lysogens if the phage integrates the bacterial genome) or become resistant to
252 phage by mutation (*i.e.*, capsule inactivation, which decreases their growth rate). We then
253 measured, over time, both the total number of cells and the proportions of lysogens.

254
255 We observed two main patterns. When prophages have low spontaneous induction rates (1 to
256 5%), they generate stable, non-costly lysogens. Consequently, phages spread slowly in the
257 bacterial population, which gives time for the phage resistant mutants to emerge and increase
258 to high frequencies. However, because these mutations are costly, lysogens slowly but
259 eventually displace them. This results in a sigmoidal-like temporal frequency of lysogens,
260 where at the end of the simulations most of the resistant population is composed of lysogens
261 (Fig 3D and lower left part of panel Figure 3 – Figure Supplement 4). These dynamics are in
262 contrast with the bell-shaped dynamics observed for high or intermediate rates of spontaneous
263 prophage induction (*i.e.*, $\geq 11\%$), where lysogens quickly invade the population but are
264 absent at the end. Such high rates correspond to unstable lysogens that quickly die due to
265 spontaneous induction of their prophages. These conditions facilitate the propagation of
266 phage throughout the population (due to fast phage amplification), and result in the rapid
267 emergence of new bacterial lysogens ($t=10$ in Fig 3D and Figure 3 – Figure Supplement 4A).
268 Becoming a lysogen can be advantageous if these cells are protected from new phage
269 infections. However, if there are high rates of prophage induction, lysogeny may become less
270 adaptive than other mechanisms of protection, e.g. receptor loss (Fig S8B). As a result, when
271 spontaneous induction rates are high and other, potentially fitter, resistant clones emerged,
272 few or no lysogens are expected to survive as they will be outcompeted (top-right areas for
273 the heatmaps in Figure 3 – Figure Supplement 4A). This is consistent with our experimental
274 results, where BJ1 clones quickly become lysogens with high induction rates which leads to
275 their removal from the population by the end of the experimental evolution.

276
277 In our simulations, the absence of capsule-inactivating mutations (resistance probability = 0,
278 rightmost column of the heatmaps in Figure 3 – Figure Supplement 4A), implies that
279 populations either become extinct (if induction rates are too high) or are completely
280 composed of lysogens. In contrast, our *in vitro* experiments revealed some resistant clones
281 that were still capsulated and non-lysogens, indicating alternative mechanisms of resistance to
282 phage. These novel clones were more frequent in populations under high phage induction

pressure (MMC), when the cost of lysogeny is high, and less frequent under growth in LB with or without citrate (Kruskal-Wallis, $dF=2$, $P=0.03$) (Figure 3). Taken together, our results show that most clones became resistant by capsule inactivation, a few by lysogenization, and others by novel mechanisms. These experimental results fit our simulations in suggesting the existence of competition between multiple phage resistance mechanisms.

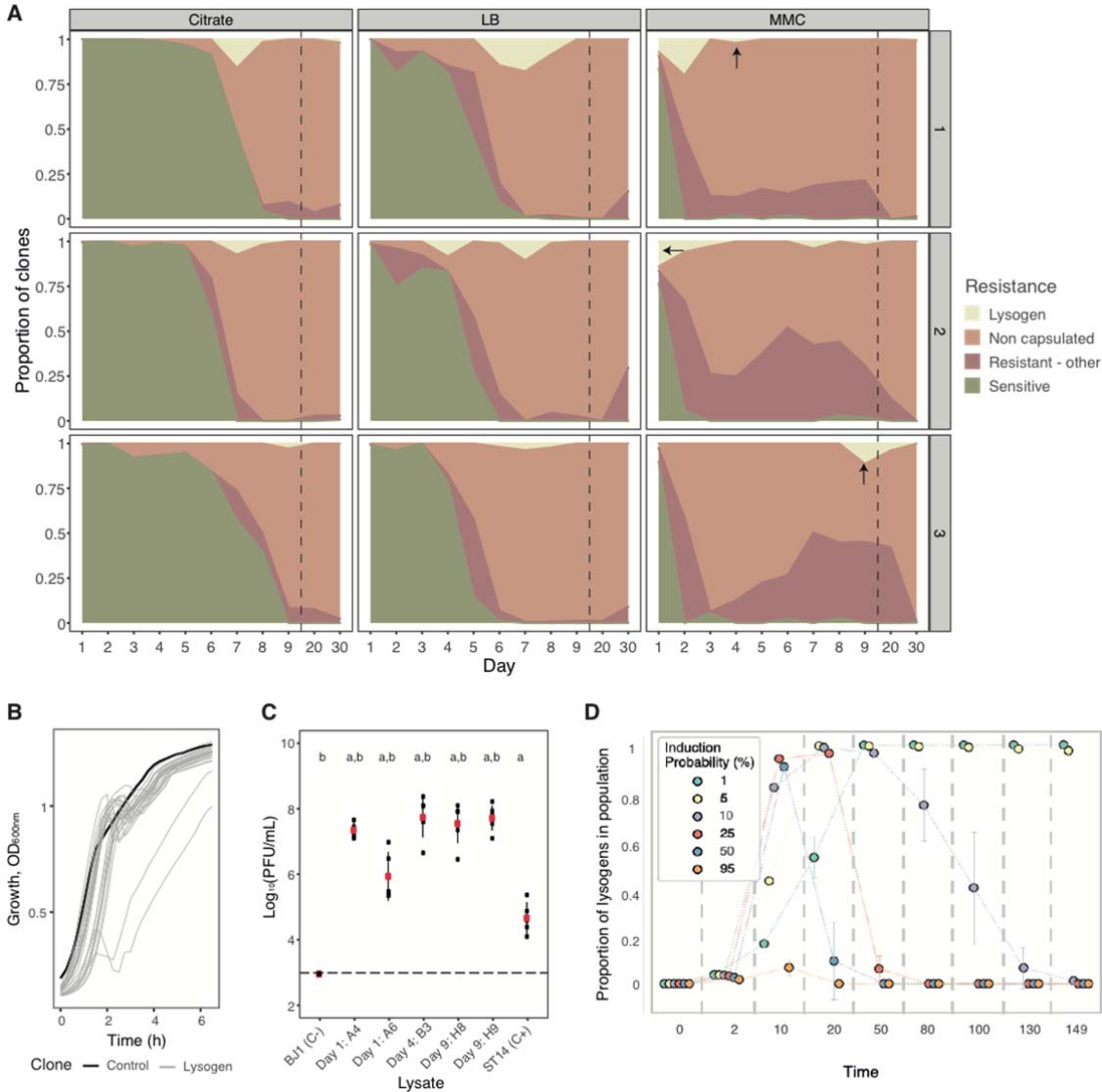


Figure 3. Evolution of resistance mechanisms in strain BJ1. **A.** Ratio of clones from each coevolving population that are susceptible (green), non-capsulated (light pink), capsulated lysogens (beige), or capsulated but resistant by other undefined mechanisms (dark pink). N.B. Dashed line indicates when x-axis, no longer follows a linear scale. Dark arrows indicate the time points from which the lysogens tested in panel C were retrieved. **B.** Growth of newly lysogenized clones reveal significant death during exponential phase (in the absence of induction), as measured by the optical density. Black line corresponds to the control, BJ1 ancestor. **C.** PFU/mL produced without induction by five selected new lysogens derived from BJ1 and isolated at day 1 for A4 and A6 (Population #2, MMC), at day 4 for B3 (Population #3, MMC) and day 9 for H8 and H9 (Population #3, MMC). Dashed line indicates the limit of detection of the essay. Each black dot represents an independent

biological replicate (independent strain lysate) and large red dots represent the mean. Error bars correspond to the standard deviation. Two-sided t-test 'a', $P < 0.001$ compared to ancestor BJ1 (negative control, C-) and 'b', $P < 0.05$ compared to ST14 (phage producer, positive control, C+). **D.** Simulated temporal dynamics of proportion of lysogens in the populations, as calculated by eVIVALDI. Each circle corresponds to the central tendency of replicate simulations, with the different colours indicating a given probability of spontaneous prophage induction (shown in the legend, values approximated to nearest major integer). The error bars correspond to the standard deviation across the replicate simulations. In the represented simulations, the probability of acquisition of a phage resistance mutation (capsule loss) is 0.001, and the fitness cost of this mutation is 10% of the bacterial growth rate, as calculated in (43).

The cost of resistance mechanisms vary with phage pressure and across time scales

To test the competitive fitness of the evolved clones having different phage-resistance mechanisms, we compared the area under growth curves of all BJ1 evolved clones isolated in the presence or in the absence of phage (Figure 4). In the first ten days of the evolution experiment, non-capsulated clones have a higher AUC than all other resistant clones in the presence of the phage and in the controls. This can be explained both by their intrinsic fitness advantage in nutrient rich environments, compared to wild type clones (43) and by their efficient resistance to phage (34, 37, 38). Hence, their fitness advantage likely drove their rapid expansion in the populations (Figure 3).

AUC analyses also revealed that lysogens are less fit than the resistant capsulated clones, in the absence of phage. However, this is not so, in the presence of phage at short evolutionary time scales. At longer time scales (after ten days of evolution), resistant capsulated clones are fitter than lysogens, in the presence of phage, supporting our previous observations that lysogeny incurs a high fitness cost. This suggests that resistant mechanisms that emerge more frequently or that are accessible in evolutionary terms, such as capsule inactivation and lysogeny could be initially selected for, but become less advantageous at longer timescales where other less costly resistance mechanisms seem to provide higher fitness. Overall, our results show a hierarchy in competitive advantage of phage resistance mechanisms, that varies across time scales and phage pressure.

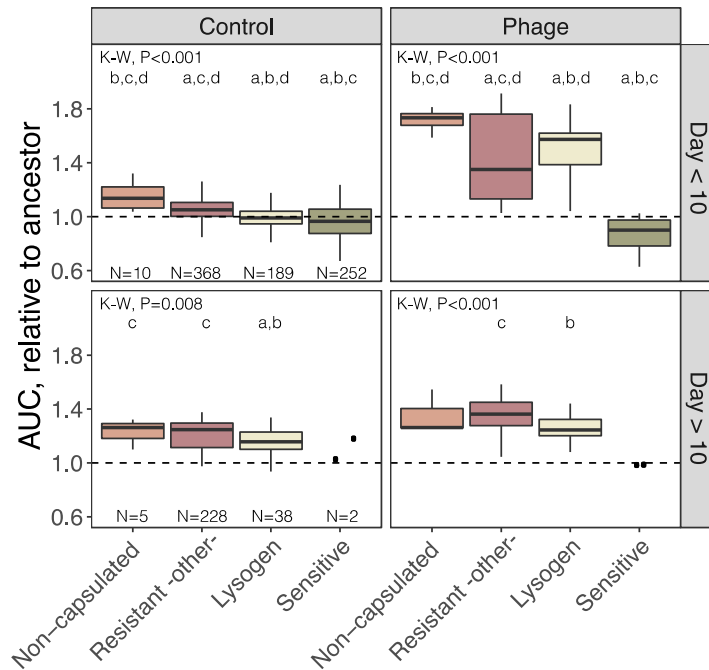


Figure 4. Growth of BJ1 resistant clones. All isolated clones that were capsulated and tested for resistance (Figure 3A and Figure 3 – Figure Supplement 1) were grown in the absence of phage (control) or with phage. One or two non-capsulated clones per day were randomly selected and included in the analyses. The area under the growth curve of each clone was estimated, and compared to that of the BJ1 ancestor (dashed line). K-W, Kruskal-Wallis test. *Post hoc* tests for significant differences across groups was calculated and p-values adjusted for multiple testing with Bonferroni correction. *a*, $P < 0.05$ difference from non-capsulated; *b*, $P < 0.05$ difference from resistant by other mechanisms; *c*, $P < 0.05$ difference from lysogens; *d*, $P < 0.05$ difference from sensitive strains.

Several changes in the receptor production play a role in resistance to phages

To identify the mechanisms of resistance to phages that involved neither receptor inactivation nor lysogeny, we characterized twelve random clones out of the 328 clones with such profiles. We measured their capsule production and resistance to purified phage lysate, either on a layer of melted agar or during growth in liquid culture. We then tested the ability of each clone to adsorb phage lysate to understand if resistance occurs prior to entering the cell. As controls, we used the ancestral strain (BJ1), as well as an $\Delta rcsB$ mutant, with reduced capsule expression, and a non-capsulated $\Delta wcaJ$ mutant (Figure 5). Additionally, we performed whole genome sequencing on all twelve resistant clones and looked for mutational targets, using the ancestral sequence as reference (Table 1).

The integration of these analyses revealed several resistance genotypes. Five independent clones had mutations in the capsule operon. Two clones (3E1 and 9G11) had frameshift mutations in a gene coding for an acyltransferase, *orf13*, and potentially leading to a change in the capsule's biochemical composition (Figure 5A, Table 1). These clones were fully

resistant to phage both in liquid and on agar, and had a diminished capsule production, comparable to the phage susceptible $\Delta rcsB$ mutant. However, phage particles could not successfully adsorb to the surface (Figure 5B). The three remaining clones had a non-synonymous mutation in *orf13* (2D2) and in *wcaJ* (9H3) and an 11 base-pair deletion in the capsule regulator *wzi* (9H7). These clones have reduced capsule expression comparable to mutations 3E1 and 9G11 in *orf13*, reduced phage adsorption and an increased resistance to phage in liquid media (Figure 5B). Surprisingly, these three clones are susceptible to phage when growing on agar. These results suggest that the effect of small capsule modifications in phage resistance might be dependent on the environment. Finally, we found no mutations in known phage defence mechanisms, such as CRISPR-Cas or restriction-modification enzymes. Taken together, our results show that there are multiple paths to resistance that involve modulating either the capsule amount or its composition.

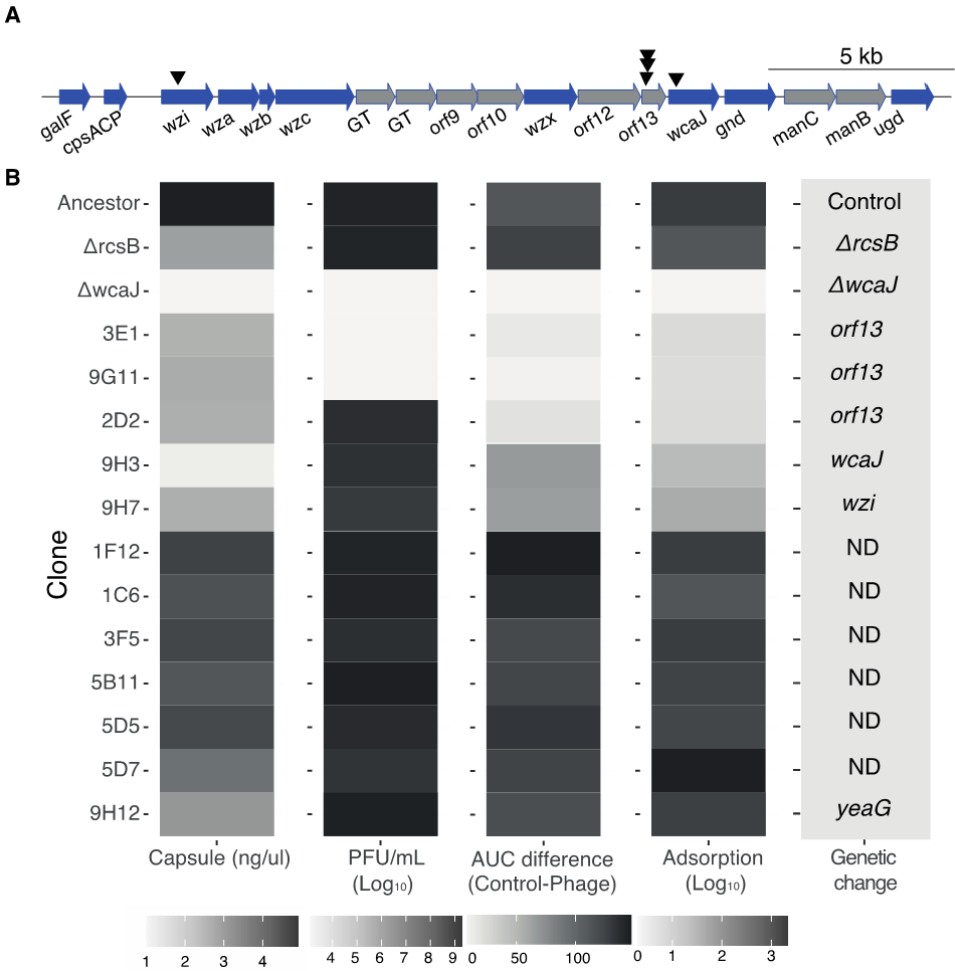


Figure 5. Characteristics of phage resistant clones. **A.** Schematic organization of the capsule operon of strain BJ1. Black triangles represent mutations observed in the capsule operon. Blue arrows indicate core genes common to all *K. pneumoniae* capsule serotypes. Grey arrows correspond to serotype-specific genes. GT stands for glycosyltransferase. The diagram was generated with genoplR package. **B.** For each clone, we evaluated the amount of capsule produced, the ability of the phage to be adsorbed and phage the sensitivity on overlay by

EOP (PFU/mL) and on liquid culture by AUC. The AUC difference accounts for the surplus of growth of the control compared to growth with phage. If the clone is resistant, the difference in AUC is ~ 0. The average of three independent replicates is shown. The experiments were performed with three independently generated lysates, when applicable. ND: none detected.

Table 1. List of mutations identified in the resistant clones sequenced. Location indicates if the mutation is found on the chromosome (C) or plasmid (P). Pop stands for population. The number of mapped sequences is also reported. Clones with less than 98% of mapped sequences are displayed in italics.

Clone	Pop	Condition	Day	Location	Position	Change	Mutation type	Annotation	Function	Mapped sequences
1C6	1	MMC	1							98.3
1F12	2	MMC	1							98.4
2D2	2	MMC	2	C	3,994,990	T→A	I110F (ATT → TTT)	<i>orf13</i>	K2 capsule gene; Polysialic acid O-acetyltransferase	98.2
3E1	1	MMC	3	C	3,995,203	(T) _{8→7}	coding (115/669 nt)	<i>orf13</i>	K2 capsule gene; Polysialic acid O-acetyltransferase	98.4
3F5	3	MMC	3	C						98.6
5B11	1	LB	5	P	34,553	A→G	intergenic (+401/-389)		hypothetical protein/hypothetical protein	98.2
				P	34,561	A→G	intergenic (+409/-381)		hypothetical protein/hypothetical protein	
5D5	2	LB	5							98.5
5D7	2	LB	5							98.6
9G11	1	LB	9	C	3,995,203	(T) _{8→9}	coding (115/669 nt)	<i>orf13</i>	K2 capsule gene; Polysialic acid O-acetyltransferase	98.3
9H7	2	Citrate	9	C	2,890,708	C→T	R121R (CGG → CGA)	<i>dcuR</i>	Transcriptional regulatory protein DcuR	98.5
				C	4,009,965	Δ11 bp	coding (245-255/630 nt)	<i>wzi</i>	K2 regulatory capsule gene	
9H3	1	Citrate	9	C	3,994,389	C→T	M61I (ATG → ATA)	<i>wcaJ</i>	UDP-glucose:undecaprenyl-phosphate glucose-1-phosphate transferase	98.5
9H12	3	Citrate	9	C	2,575,329	C→T	D615N (GAC → AAC)	<i>yeaG</i>	Protein kinase YeaG	98.6
				P	23,432	G→A	R34Q (CGG → CAG)	<i>soj</i>	Phage cox protein (PF10743), annotated as plasmid-partitioning	

Interestingly, the remaining seven clones that were identified in our initial screens to be resistant seem to be susceptible to phage lysate in all subsequent tests. Despite their marginally lower capsule production, we could not detect mutations in their genome relative to their ancestors (except for one clone with an intergenic mutation). To discard the possibility that this could be due to a problem in our initial screen for resistant clones, we returned to the original glycerol stocks and retested these clones for their resistance to phage during growth in liquid (*i.e.* the same conditions as the screen) (Figure 6). To avoid a possible loss of the phenotype due to culture passaging, we initiated the growth curves directly from the glycerol stock without performing a preconditioning culture, that is, an acclimation step. When the culture reached OD ~0.2, we added the phage lysate. We observed that the cultures grown directly from the stocks were resistant to phage. The difference between the clones from the glycerol stock and those sequenced is that the sequenced clones underwent two extra

round of LB passaging without phage pressure. Hence, these results suggest that transient resistance to phages can emerge without mutations (Figure 6 and Figure 6– Figure Supplement 1).

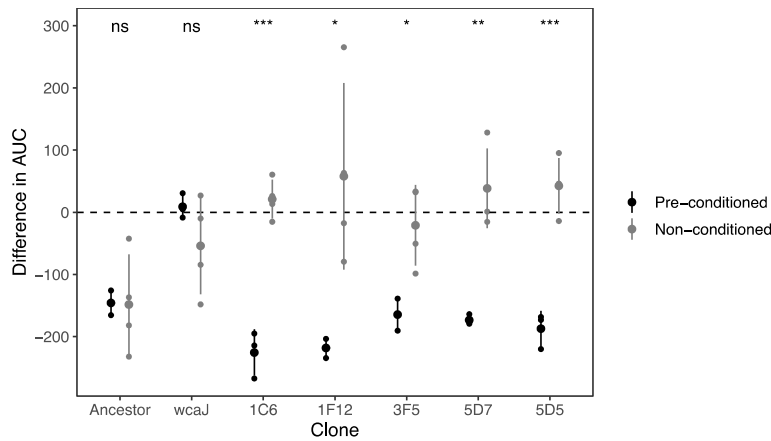


Figure 6. Transient resistance to phages. The difference in the area under the curve (AUC) represents the effect of adding phage to a growing culture as estimated by the difference in growth curve in the absence of phage and with phage (Figure 6 – Figure Supplement 1). Values below 0 indicate strains are sensitive to phage, and values close to 0 indicate that there is no effect of adding phage to the culture. Non-conditioned clones are those directly grown from glycerol stock, whereas pre-conditioned clones, had been reisolated twice, and grown overnight prior to performing the growth analyses. The ancestor, BJ1, sensitive, and the non-capsulated mutant ($\Delta wcaJ$), are included as controls for the difference in culture conditions. Each small dot represents an independent biological replicate. Statistics represent t-tests to check from differences between clones directly from stock and those sequenced (after two passages in LB). ns means non-significant, * $P < 0.05$, ** $P < 0.01$ and *** $P < 0.001$.

Receptor modifications but not lysogenization provide cross-resistance to other phages

We sought to test whether resistance to phages from ST14 could result in resistance to phages produced by other strains. To test potential cross-resistance between lysates, we produced phage lysates from strains 03-9138, ST17 and T69, all of which were previously shown to successfully infect BJ1 (34). We first infected the non-lysogenized BJ1 clones that are capsulated and resistant to ST14 phages. We observed that these clones were also resistant to the phage in lysates of strain 03-9138 and ST17 but not those of T69, suggesting that one of the phages of T69 may not use the capsule as a primary receptor (Figure 7A and Figure 7 – Figure Supplement 1). Cross-resistance could result from phages sharing a specificity for the capsule serotype (44). The strains from which we produced the lysate have very dissimilar prophages, as determined by wGRR, a measure of phage similarity for all intact phages –see Methods- (wGRR<0.25, Figure 7 – Figure Supplement 1B, (34)). Yet, 23 proteins from these phages showed sequence identity higher than 50% with proteins present in the two ST14 phages (Figure 7 – Figure Supplement 1B). The functional analyses of these proteins using

pVOG revealed that some are structural proteins potentially involved in infection (e.g., tail proteins) (Figure 7 – Figure Supplement 1D). They may provide different phages with similar tropism, thereby explaining the observed cross-resistance among lysogens of the same serotype.

We then tested whether the lysogenized BJ1 clones, resistant to ST14 lysate, were also resistant to other lysates. To do so, we assessed plaque formation on lysogen lawns rather than growth inhibition, as these new lysogens already exhibited significant cell death due to phage outburst (Figure 3B). Despite similarities between phages across lysates, BJ1 lysogens were only resistant to ST14 lysate, remaining sensitive to lysates produced by other strains (Figure 7B). Hence, and in contrast with the cross-resistance profile of clones with capsule modifications, integration of ST14 phages into BJ1 does not result in resistance to super infection against a larger array of serotype-specific phages.

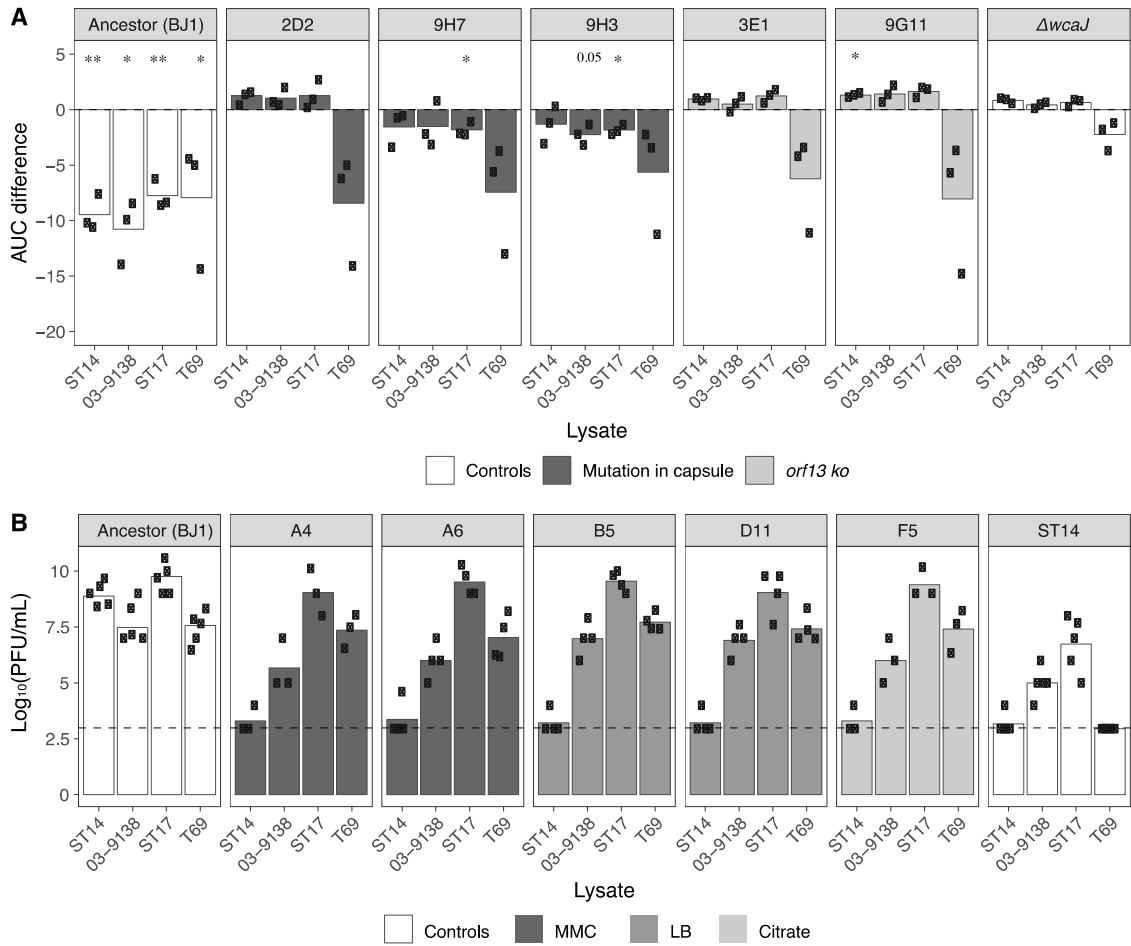


Figure 7. Cross resistance to phages from other lysates. **A.** The area under the curve for capsulated (and non-lysogenized) resistant clones was calculated. The AUC of control cultures with LB was subtracted from those that were challenged with phage lysates. (Growth curves are shown in Figure 7 – Figure Supplement 1A). Each dot represents an independent assay. One-sample t-tests were performed to test the difference from 0 (growth in LB). * $P < 0.05$; ** $P < 0.01$ **B.** PFU/mL of three independently generated lysates on lawns of new BJ1 lysogens from different evolutionary treatments. Lysogens A4 and A6 evolved in MMC and were isolated at day 1, lysogens B5 and D111 evolved in LB and were isolated at day 6 and 7 respectively, and clone F5 evolved in citrate and was isolated at day 7. Each black dot represents an independent biological replicate. The dashed line represents the limit of detection of the assay.

DISCUSSION

We explored how temperate phages drive population dynamics during coevolution between two *K. pneumoniae* strains under different degrees of parasite pressure. Based on theoretical works (45) and direct 24-hour competitions, we hypothesized that phage sensitive BJ1 would coexist with polylysogenic ST14 in conditions with low phage infection but would be outcompeted fast in conditions of high phage concentration. We however observed that both ST14 and BJ1 are present in all populations. The varying relative frequency of the two strains along time suggests continuing co-evolution, since the initial drop in phage-susceptible BJ1 populations correlates with an increase of phage production, and then stabilization of both phage and BJ1 populations, prior to a second drop in BJ1 frequency. In populations evolving in the environment with MMC, BJ1 populations dropped faster than in the other conditions. This could be linked to a faster capsule inactivation. Changes in the *Klebsiella* capsule are a primary mechanism of resistance to temperate phages, as shown for virulent phages (37, 38, 46, 47). More broadly, fast inactivation of the capsule confirms that alteration of the host recognition determinants frequently result in the protection of bacterial populations against phage (48-50). However, after 6 days of co-evolution, the frequencies of both strains in MMC reached an equilibrium. This also resulted in a higher frequency of BJ1 strain at the end of the evolution experiment, compared to populations which were initially exposed to less phage pressure. High BJ1 frequencies in these populations are potentially linked to the emergence of diverse resistance mechanisms imposing lower fitness costs (Figure 4). Indeed, non-capsulated clones are fitter at early stages of the coevolution, but capsulated non-lysogenized BJ1 resistant clones may outcompete other resistant BJ1 at longer evolutionary time scales.

Lysogenization often renders bacteria resistant to phages due to superinfection exclusion (51, 52). Our previous work revealed frequent lysogenization of BJ1 when exposed to highly concentrated lysate of ST14 (34), as expected from experimental (53) and modelling studies (42). We now show that lysogenization is not a stable mechanism of defence in this system

(Figure 3A). This is because it results in high rates of spontaneous phage induction that lead to cell death. Similar observations were made with *E. coli* in a murine model in which high induction rates of phage lambda decreased the fitness of lysogens (23). Frazão *et al* also observed that after lysogenization, phage induction was very high, however, this was followed by progressive domestication (33), suggesting that the cost of some resistant mechanisms can be overcome. In the present work, the producing strain is a polylysogen, which could further complicate the acquisition of resistance since full protection requires multiple lysogenization events (one for each phage). For instance, lysogenic conversion was less frequent (~50% less) when a non-lysogenic *P. aeruginosa* was competed against a polylysogenic strain, compared to conditions when it was exposed to a single-lysogenized strain (31). Overall, lysogeny is disfavoured as a mechanism of phage resistance when the rates of spontaneous induction are high or when bacteria are targeted by multiple different phages, or when other less costly alternative resistant mechanisms may emerge.

A major finding of our work is that the type of the resistance mechanisms changes across evolutionary time scales. At first, resistance emerged quickly by the loss of capsule production because functional inactivation can be achieved in many ways (Supplementary File 2, (40, 41, 54)). At later stages, resistance may emerge by changes in composition or expression of the capsule, which can outcompete both lysogens and non-capsulated clones. The emergence of these mechanisms later in the experiment suggest that such mutations are under more limited supply than those resulting in capsule loss. This suggests that either long-term adaptation requires a small pool of rare mutations, contrary to gene inactivation that can be achieved in multiple ways, or that these adaptive paths are more complex, e.g. require multiple steps.

Surprisingly, our study revealed that some phage-resistant clones reverted to susceptibility after two passages in the absence of phage pressure. Yet, the sequence of these clones failed to reveal any mutations that could explain the phenotypic change. An increasing number of recent reports suggest that phage resistance could often be transient. For instance, Hesse and colleagues sequenced 57 different clones of *K. pneumoniae* resistant to a virulent phage and found that almost half of them lacked identifiable mutations (37). Our clones could be transiently resistant because the nucleotide sequence of the gene *wcaJ* of the K2 capsule have short simple sequence repeats (SSR) whose changes are difficult to detect with the current genome assemblers and variant calling software. SSR are known mutational hotspots in

rapidly evolving traits and their changes are easily reversible (55). In agreement with this hypothesis, we found that capsule inactivation in ST14 is associated with an insertion of a thymine among a repeat of thymine residues (Supplementary File 2). Other, non-genetic mechanisms of transient resistance to phages have also been described (56-59). One is the epigenetic-based resistance based on DNA modifications, such as methylation. This was previously shown to regulate the length of the O-antigen length by phase variation in *Salmonella enterica*, and resulted in transient phage resistance (57). Additionally, transient cell wall shedding in filamentous actinobacteria, *B. subtilis* and *E. coli* (58) and conversion to cell wall-deficient L-forms in *Listeria monocytogenes* (59) can lead to transient phage resistance. An analogous process in *K. pneumoniae* could involve the shedding of the capsule in response to phage pressure, resulting in a state of reduced phage adsorption and limited infection. Such non-genetic protective changes are comparable to inducible immune responses (CRISPR-Cas) that incur in lower fitness costs relative to other constitutive changes such as permanent loss of receptors (49). Here, we show that at a longer evolutionary time scale, non-genetic modifications or inducible resistance can emerge. Contrary to a constitutive inactivation of the capsule, non-genetic mechanisms do not result in added cost and the bacteria can revert to susceptibility once phage pressure is relieved.

Both the efficiency and fitness costs of phage-resistance mechanisms are context-dependent, as they can impose trade-offs in different environmental conditions (60). We found that some mutants were only resistant to phages in liquid media, *i.e.*, in the environment where they evolved, but remained fully sensitive to the same phages when growing on agar. This recapitulates phage-resistant *Pseudomonas syringae* evolved *in vitro* that did not display a fitness advantage compared to phage-sensitive cells, when grown on a plant surface in the presence of phage (61). These results are unexpected given previous studies showing that phage-sensitive bacteria are able to survive phage attacks in structured environments (agar, gut or plant surface) due to the existence of refuges where sensitive cells may evade the phage (28, 62-65). However, survival in refuges is often contingent to the presence of other phage resistant clones, or enhanced phenotypic resistance in structured environments due to reduced receptor expression (66). A plausible explanation could be that in well-shaken liquid, phage-bacterium interactions are unstable, compared to interactions on agar (67). If this is true, then less capsulated mutants could attain a higher level of resistance in liquid than in solid. Yet, resistance is not necessarily linked to a mere reduction in the production of capsule because the $\Delta rcsB$ mutant that produces less capsule remains equally sensitive to phage in both liquid

548 and agar (Figure 5). Taken together, our results highlight the complexity of the outcomes of
549 bacterial interactions when they are affected by prophages.
550

551

552 MATERIALS AND METHODS

553

554 **Bacterial strains and growth conditions.** BJ1 (ENA : [SAMEA4968482](#)) and ST14 (ENA:
555 [SAMN22024794](#)) are two phylogenetically-distant *K. pneumoniae*, both bearing the K2
556 capsule serotype. Bacteria were grown at 37° in Luria-Bertani (LB) agar plates or in 4 mL of
557 liquid broth under vigorous shaking (250 rpm). Chloramphenicol (30 µg/ml) and
558 trimethoprim (100 µg/ml) were used to select for strain BJ1 and ST14 respectively.

559 **Competition calculations.** Calculations of B_{ij} , $C_i(j)$ were performed as reported in (68). (i)
560 *Unidirectional mixing-effect parameter $C_i(j)$.* The effect of mixing two strains i and j on the
561 population yield during growth of focal strain i was quantified by the one-way mixing effect
562 parameter $C_i(j)$. To calculate this parameter, the expected log₁₀-transformed yield of strain i
563 based on pure-culture performance (corrected for the frequency at which strain i was added)
564 was subtracted from its actual log-transformed yield during competition with strain j .

$$C_i(j) = \log_{10}\left(\frac{N_i(j, t_{24})}{N_i(j, t_0)}\right) - \log_{10}\left(\frac{N_i(t_{24})}{N_i(t_0)}\right)$$

565

566 Positive $C_i(j)$ values indicate that strain i grew to a higher population size in the experiments
567 in the presence of strain j than in pure culture, whereas a negative value indicates that mixing
568 with j negatively affected growth yield of i . (ii) *Bidirectional mixing effect parameter B_{ij} .* B_{ij}
569 is the difference between the actual total (log₁₀-transformed) group cell count in a mix of
570 strains i and j and the value expected from pure culture performance of the same strains
571 (corrected for initial frequencies of each strain).

$$B_{ij} = \log\left(\frac{\frac{N_i(j, t_{24})}{2} + \frac{N_j(i, t_{24})}{2}}{\frac{N_i(t_{24})}{2} + \frac{N_j(t_{24})}{2}}\right)$$

572 Positive and negative B_{ij} values indicate that total productivity is higher or lower,
573 respectively, than expected from pure culture performance.

574

575 **Coevolution experiment.** Three clones from each strain were used to inoculate overnight
576 cultures, which were then diluted at 1:100 and used to initiate the three independent mixed
577 populations in a ratio 1:1, in a final volume of 4 mL. Each of the three mixed populations

evolved in three different environments: (i) LB, (ii) LB supplemented with 0.2% citrate and (iii) LB with mytomycin C (MMC, 0.1 $\mu\text{g}/\text{mL}$). Cultures were allowed to grow for 24 hours at 37°C and diluted again to 1:100 in fresh media. This was repeated for 30 days. Each day, each independently evolving population was plated and serially diluted. CFUs were counted (3 plates per sample) and the emergence of non-capsulated mutants was recorded. Non-capsulated mutants are easily visualized by the naked eye as mutants produce smaller, rough and translucent colonies.

Phage experiments. (i) *Growth curves*: 200 μL of diluted overnight cultures of *Klebsiella* spp. (1:100 in fresh LB) were distributed in a 96-well plate. Cultures were allowed to reach OD = 0.2 and either mitomycin C to 1 $\mu\text{g}/\text{mL}$ or 20 μL of PEG-precipitated induced and filtered supernatants at 2×10^8 PFU/mL was added. Growth was then monitored until late stationary phase. (ii) *PEG-precipitation of phages*. Overnight cultures were diluted 1:500 in fresh LB and allowed to grow until OD = 0.2. Mitomycin C was added to final 5 $\mu\text{g}/\text{mL}$. After 4h hours at 37°C, cultures were centrifuged at 4000 rpm and the supernatant was filtered through 0.22 μm . Filtered supernatants were mixed with chilled PEG-NaCl 5X (PEG 8000 20% and 2.5M of NaCl) and mixed through inversion. Phages were allowed to precipitate for 15 min and pelleted by centrifugation 10 min at 13000 rpm at 4°C. The pellets were dissolved in TBS (Tris Buffer Saline, 50 mM Tris-HCl, pH 7.5, 150 mM NaCl). (iii) *Calculating plaque forming units (PFU)*. Overnight cultures of susceptible or tested strains were diluted 1:100 and allowed to grow until OD = 0.8. 250 μL of bacterial cultures were mixed with 3 mL of top agar (0.7% agar) and poured into prewarmed LB plates. Plates were allowed to dry before spotting serial dilutions of induced PEG-precipitated phages. Plates were left overnight at room temperature and phage plaques were counted. (iv) *Phage adsorption*. Adsorption of phage particles to the cell surface was performed as previously described (37). Briefly, each resistant clone was grown until OD ~0.35. One ml of each culture was transferred to separate wells in a 24-well plate, to which 10 μL of filtered phage lysate (ca. 5×10^6 phage particles) was added. The mix was allowed to sit for 2 minutes at room temperature prior to incubation at 37°C for 15 min with shaking at 140 rpm. Phage adsorption was measured by quantifying the free phage remaining in solution, after centrifugation for 10 minutes at 10000rpm, to get rid of bacterial cells. The supernatant was serially diluted and non-adsorbed phage was quantified by spot titer on a bacterial lawn of strain BJ1. Finally, to quantify how much phage was adsorbed, the non-adsorbed phage was subtracted from the initial amount of phage added to the culture.

Sequencing. (i) *Genomes of phage resistant clones.* Single clones were allowed to grow overday in LB supplemented with 0.7mM EDTA, to limit capsule production. We performed DNA extraction with the guanidium thiocyanate method, with few modifications (69). RNase A treatment (37°C, 30min) was performed before DNA precipitation. Each clone (n=15) was sequenced by Illumina with 150pb paired-end reads, yielding approximately 1 Gb of data per clone. The reads were compared to the reference genome using *breseq* v0.33.2, default parameters. (ii) *wcaJ* gene. PCR of *wcaJ* was performed using the primers that hybridized 150 base pairs upstream and downstream of the *wcaJ* gene; K2.*wcaJ*.150-5 (5'-GGCGTTCCAGCAAGGGTTATC -3') and K2.*wcaJ*.150-3 (5'-ACGTTCGCGCTTAAATGTG-3'), respectively. To allow full coverage of the gene, PCR products were also sequenced with primer K2.*wcaJ*.inseq-5 (5'-CTGGGTCTTTACAGAGGAATC-3'). PCR products were sequenced by Sanger and analysed using *APe*.

Capsule quantification. The bacterial capsule was extracted as described in (70). Briefly, 500 µL of an overnight culture was adjusted to OD of 2 and mixed with 100 µL of 1% Zwittergent 3-14 detergent in 100 mM citric acid (pH 2.0) and heated at 56°C for 20 minutes. Afterwards, it was centrifuged for 5 min at 14,000 rpm and 300 µL of the supernatant was transferred to a new tube. Absolute ethanol was added to a final concentration of 80% and the tubes were placed on ice for 20 minutes. After a second wash with ethanol at 70%, the pellet was dried and dissolved in 250 µL of distilled water. The pellet was then incubated for 2 hours at 56°C. Polysaccharides were then quantified by measuring the amount of uronic acid, as described in (71). A 1,200 µL volume of 0.0125 M tetraborate in concentrated H₂SO₄ was added to 200 µL of the sample to be tested. The mixture was vigorously vortexed and heated in a boiling-water bath for 5 min. The mixture was allowed to cool, and 20 µL of 0.15% 3-hydroxydiphenol in 0.5% NaOH was added. The tubes were shaken, and 100 µL were transferred to a microtiter plate for absorbance measurements (520 nm). The uronic acid concentration in each sample was determined from a standard curve of glucuronic acid.

Citrate quantification. 24 hour cultures of BJ1, ST14, their coculture, or blank tubes with citrate, were centrifuged for 10 minutes at 4000 rpm and the supernatant was sterilized with 0.22 µm filter, prior to deproteination by centrifugation in an Amicon tube (10 kDa). Citrate concentration was measured using Citrate assay kit (Sigma-Aldrich MAK333).

Individual-based simulations of bacteria-phage interactions

Simulations were performed based on the model described in (42). Briefly, both bacterial cells and phage particles are independent individuals on an environment represented as a two-dimensional grid. The environment is simulated as well-mixed, meaning that positions of bacteria and phage are randomized at each iteration. Bacterial death can be intrinsic (e.g., of old age) or explicit (e.g., lysed by phage). Bacteria can resist phage infection by acquiring a mutation that mimics capsule loss (at varying rates, with a varying fitness cost, see results). Upon phage infection, phage can either follow a lytic cycle or a lysogenic one, according to a stochastic decision defined by the parameters `LysogenyAlpha` and `LysogenyKappa`, that takes into consideration the density of nearby phages. When lysogenized, bacteria become insensitive to new phage infections, but the integrated prophage can excise (and thus lead to death of this specific cell) at varying frequencies (see results). The simulations we explored are initiated with 10000 bacterial cells, and 1000 phage particles are added into the environment at the beginning of the simulation. For each condition explored (varying the probability of phage induction, the probability of bacteria acquiring a phage resistance mutation, and the cost of this mutation), we performed 30 replicate simulations, each running for 150 iterations. The values presented in the results correspond to the median of the 30 replicate simulations, for each condition. The set of parameters explored, that are relevant for the questions in this study, are shown in Text S1. Other mechanisms that can be simulated in eVIVALDI (e.g, transduction) were not used in these simulations.

wGRR calculations. Phage similarity was calculated as described in (34). Briefly, we searched for sequence similarity between all proteins of all phages using `mmseqs2` (72) with the sensitivity parameter set at 7.5. The results were filtered with the following parameters: e-value lower than 0.0001, at least 35% identity between amino acids, and a coverage of at least 50% of the proteins. The filtered hits were used to compute the set of bi-directional best hits (bbh) between each phage pair. This was then used to compute a score of gene repertoire relatedness for each pair of phage genomes, weighted by sequence identity, computed as following:

$$\text{wGRR}_{A,B} = \sum_i \frac{id(A_i, B_i)}{\min(A, B)}$$

where A_i and B_i is the pair i of homologous proteins present in A and B (containing respectively $\#A$ and $\#B$ proteins), $\text{id}(A_i, B_i)$ is the percent sequence identity of their alignment, and $\min(A, B)$ is the total number of proteins of the smallest prophage, *i.e.* the one encoding the smallest number of proteins (A or B). wGRR varies between zero and one. It amounts to zero if there are no orthologs between the elements, and one if all genes of the smaller phage have an ortholog 100% identical in the other phage. Hence, the wGRR accounts for both frequency of homology and degree of similarity among homologs.

REFERENCES

1. Koskella B, Brockhurst MA. Bacteria-phage coevolution as a driver of ecological and evolutionary processes in microbial communities. *Fems Microbiol Rev.* 2014;38(5):916-31.
2. Pedersen AB, Fenton A. Emphasizing the ecology in parasite community ecology. *Trends Ecol Evolution.* 2007;22(3):133-9.
3. Lefèvre T, Lebarbenchon C, Gauthier-Clerc M, Missé D, Poulin R, Thomas F. The ecological significance of manipulative parasites. *Trends Ecol Evolution.* 2009;24(1):41-8.
4. Brussow H, Hendrix RW. Phage genomics: Small is beautiful. *Cell.* 2002;108(1):13-6.
5. Suttle CA. Marine viruses - major players in the global ecosystem. *Nat Rev Microbiol.* 2007;5(10):801-12.
6. Touchon M, Bernheim A, Rocha EPC. Genetic and life-history traits associated with the distribution of prophages in bacteria. *Isme J.* 2016;10(11):2744-54.
7. Godeke J, Paul K, Lassak J, Thormann KM. Phage-induced lysis enhances biofilm formation in *Shewanella oneidensis* MR-1. *Isme J.* 2011;5(4):613-26.
8. Sullivan MB, Coleman ML, Weigle P, Rohwer F, Chisholm SW. Three *Prochlorococcus* cyanophage genomes: signature features and ecological interpretations. *PLoS Biol.* 2005;3(5):e144.
9. Busby B, Kristensen DM, Koonin EV. Contribution of phage-derived genomic islands to the virulence of facultative bacterial pathogens. *Environ Microbiol.* 2013;15(2):307-12.
10. Fasano A, Baudry B, Pumphlin DW, Wasserman SS, Tall BD, Ketley JM, et al. *Vibrio cholerae* produces a second enterotoxin, which affects intestinal tight junctions. *Proc Natl Acad Sci U S A.* 1991;88(12):5242-6.
11. Varani AM, Monteiro-Vitorello CB, Nakaya HI, Van Sluys MA. The role of prophage in plant-pathogenic bacteria. *Annu Rev Phytopathol.* 2013;51:429-51.
12. Winstanley C, Langille MG, Fothergill JL, Kukavica-Ibrulj I, Paradis-Bleau C, Sanschagrin F, et al. Newly introduced genomic prophage islands are critical determinants of *in vivo* competitiveness in the Liverpool Epidemic Strain of *Pseudomonas aeruginosa*. *Genome Res.* 2009;19(1):12-23.
13. Bobay LM, Touchon M, Rocha EP. Pervasive domestication of defective prophages by bacteria. *Proc Natl Acad Sci U S A.* 2014;111(33):12127-32.
14. Nakayama K, Takashima K, Ishihara H, Shinomiya T, Kageyama M, Kanaya S, et al. The R-type pyocin of *Pseudomonas aeruginosa* is related to P2 phage, and the F-type is related to lambda phage. *Mol Microbiol.* 2000;38(2):213-31.
15. Bondy-Denomy J, Qian J, Westra ER, Buckling A, Guttman DS, Davidson AR, et al. Prophages mediate defense against phage infection through diverse mechanisms. *Isme J.* 2016;10(12):2854-66.

16. Li XY, Lachnit T, Fraune S, Bosch TCG, Traulsen A, Sieber M. Temperate phages as self-replicating weapons in bacterial competition. *J R Soc Interface*. 2017;14(137):20170563.
17. Joo J, Gunny M, Cases M, Hudson P, Albert R, Harvill E. Bacteriophage-mediated competition in *Bordetella* bacteria. *P Roy Soc B-Biol Sci*. 2006;273(1595):1843-8.
18. Harrison E, Brockhurst MA. Ecological and Evolutionary Benefits of Temperate Phage: What Does or Doesn't Kill You Makes You Stronger. *Bioessays*. 2017;39(12):1700112.
19. Wendling CC, Refardt D, Hall AR. Fitness benefits to bacteria of carrying prophages and prophage-encoded antibiotic-resistance genes peak in different environments. *Evolution*. 2021;75(2):515-28.
20. Haaber J, Leisner JJ, Cohn MT, Catalan-Moreno A, Nielsen JB, Westh H, et al. Bacterial viruses enable their host to acquire antibiotic resistance genes from neighbouring cells. *Nat Commun*. 2016;7:13333.
21. Bondy-Denomy J, Davidson AR. When a virus is not a parasite: the beneficial effects of prophages on bacterial fitness. *J Microbiol*. 2014;52:235-42.
22. Bossi L, Fuentes JA, Mora G, Figueroa-Bossi N. Prophage contribution to bacterial population dynamics. *J Bacteriol*. 2003;185(21):6467-71.
23. De Paepe M, Tournier L, Moncaut E, Son O, Langella P, Petit MA. Carriage of lambda Latent Virus Is Costly for Its Bacterial Host due to Frequent Reactivation in Monoxenic Mouse Intestine. *PLoS Genet*. 2016;12(2):e1005861.
24. Gama JA, Reis AM, Domingues I, Mendes-Soares H, Matos AM, Dionisio F. Temperate Bacterial Viruses as Double-Edged Swords in Bacterial Warfare. *Plos One*. 2013;8(3):e59043.
25. Nanda AM, Thormann K, Frunzke J. Impact of spontaneous prophage induction on the fitness of bacterial populations and host-microbe interactions. *J Bacteriol*. 2015;197(3):410-9.
26. Brockhurst MA, Morgan AD, Fenton A, Buckling A. Experimental coevolution with bacteria and phage *The Pseudomonas fluorescens* - Phi 2 model system. *Infect Genet Evol*. 2007;7(4):547-52.
27. Fazzino L, Anisman J, Chacon JM, Heineman RH, Harcombe WR. Lytic bacteriophage have diverse indirect effects in a synthetic cross-feeding community. *Isme J*. 2020;14(1):123-34.
28. Lourenco M, Chaffringeon L, Lamy-Besnier Q, Pedron T, Campagne P, Eberl C, et al. The Spatial Heterogeneity of the Gut Limits Predation and Fosters Coexistence of Bacteria and Bacteriophages. *Cell Host Microbe*. 2020;28(3):390-405.
29. Weinbauer MG. Ecology of prokaryotic viruses. *Fems Microbiol Rev*. 2004;28(2):127-81.
30. Weinbauer MG, Rassoulzadegan F. Are viruses driving microbial diversification and diversity? *Environ Microbiol*. 2004;6(1):1-11.
31. Burns N, James CE, Harrison E. Polylysogeny magnifies competitiveness of a bacterial pathogen *in vivo*. *Evol Appl*. 2015;8(4):346-51.
32. Davies EV, James CE, Kukavica-Ibrulj I, Levesque RC, Brockhurst MA, Winstanley C. Temperate phages enhance pathogen fitness in chronic lung infection. *Isme J*. 2016;10(10):2553-5.
33. Frazão N, Konrad A, Amicone M, E. S, Güleresi D, Lässig M, et al. Two modes of evolution shape bacterial strain diversity in the mammalian gut for thousands of generations. *Nat Commun*. 2022;13(1):5604
34. de Sousa JAM, Buffet A, Haudiquet M, Rocha EPC, Rendueles O. Modular prophage interactions driven by capsule serotype select for capsule loss under phage predation. *Isme J*. 2020;14(12):2980-96.
35. Shafia F, Thompson TL. Calcium ion requirement for proliferation of bacteriophage phi mu-4. *J Bacteriol*. 1964;88(2):293-6.

36. León-Félix J, Villicaña C. The Impact of Quorum Sensing on the Modulation of Phage-Host Interactions. *J Bacteriol.* 2021;203(11):e00687-20.
37. Hesse S, Rajaure M, Wall E, Johnson J, Bliskovsky V, Gottesman S, et al. Phage Resistance in Multidrug-Resistant *Klebsiella pneumoniae* ST258 Evolves via Diverse Mutations That Culminate in Impaired Adsorption. *Mbio.* 2020;11(1):e02530-19.
38. Tan D, Zhang Y, Qin J, Le S, Gu J, Chen LK, et al. A Frameshift Mutation in *wcaJ* Associated with Phage Resistance in *Klebsiella pneumoniae*. *Microorganisms.* 2020;8(3):378.
39. Venturini C, Ben Zakour NL, Bowring B, Morales S, Cole R, Kovach Z, et al. Fine capsule variation affects bacteriophage susceptibility in *Klebsiella pneumoniae* ST258. *Faseb J.* 2020;34(8):10801-17.
40. Chiarelli A, Cabanel N, Rosinski-Chupin I, Zongo PD, Naas T, Bonnin RA, et al. Diversity of mucoid to non-mucoid switch among carbapenemase-producing *Klebsiella pneumoniae*. *Bmc Microbiol.* 2020;20(1):325.
41. Haudiquet M, Buffet A, Rendueles O, Rocha EPC. Interplay between the cell envelope and mobile genetic elements shapes gene flow in populations of the nosocomial pathogen *Klebsiella pneumoniae*. *Plos Biol.* 2021;19(7):e3001276.
42. de Sousa JAM, Rocha EPC. Environmental structure drives resistance to phages and antibiotics during phage therapy and to invading lysogens during colonisation. *Scientific Reports.* 2019;9(1):3149.
43. Buffet A, Rocha EPC, Rendueles O. Nutrient conditions are primary drivers of bacterial capsule maintenance in *Klebsiella*. *P Roy Soc B-Biol Sci.* 2021;288(1946):20202876.
44. Beamud B, García-González N, Gómez-Ortega M, González-Candelas F, Domingo-Calap P, Sanjuan R. Genetic determinants of host tropism in *Klebsiella* phages. *Cell Rep.* 2022;42(2):112048.
45. Brown SP, Le Chat L, De Paepe M, Taddei F. Ecology of microbial invasions: Amplification allows virus carriers to invade more rapidly when rare. *Curr Biol.* 2006;16(20):2048-52.
46. Cai RP, Wang G, Lee S, Wu M, Cheng MJ, Guo ZM, et al. Three Capsular Polysaccharide Synthesis-Related Glucosyltransferases, GT-1, GT-2 and WcaJ, Are Associated With Virulence and Phage Sensitivity of *Klebsiella pneumoniae*. *Front Microbiol.* 2019;10:1189.
47. Majkowska-Skrobek G, Markwitz P, Sosnowska E, Lood C, Lavigne R, Drulis-Kawa Z. The evolutionary trade-offs in phage-resistant *Klebsiella pneumoniae* entail cross-phage sensitization and loss of multidrug resistance. *Environ Microbiol.* 2021;23(12):7723-40.
48. Mutalik VK, Adler BA, Rishi HS, Piya D, Zhong C, Koskella B, et al. High-throughput mapping of the phage resistance landscape in *E. coli*. *PLoS Biol.* 2020;18(10):e3000877.
49. Westra Edze R, van Houte S, Oyesiku-Blakemore S, Makin B, Broniewski Jenny M, Best A, et al. Parasite Exposure Drives Selective Evolution of Constitutive versus Inducible Defense. *Curr Biol.* 2015;25(8):1043-9.
50. Shaer Tamar E, Kishony R. Multistep diversification in spatiotemporal bacterial-phage coevolution. *Nat Commun.* 2022;13(1):7971.
51. Cumby N, Edwards AM, Davidson AR, Maxwell KL. The bacteriophage HK97 gp15 moron element encodes a novel superinfection exclusion protein. *J Bacteriol.* 2012;194:5012-9.
52. Susskind MM, Wright A, Botstein D. Superinfection exclusion by P22 prophage in lysogens of *Salmonella typhimurium*. IV. Genetics and physiology of sieB exclusion. *Virology.* 1974;2:367-84.
53. Zeng L, Skinner SO, Zong C, Sippy J, Feiss M, Golding I. Decision Making at a Subcellular Level Determines the Outcome of Bacteriophage Infection. *Cell.* 2010;141(4):682-91.

54. Nucci A, Rocha EPC, Rendueles O. Adaptation to novel spatially-structured environments is driven by the capsule and alters virulence-associated traits. *Nat Commun.* 2022;13(1):4751.
55. Moxon ER, Rainey PB, Nowak MA, Lenski RE. Adaptive evolution of highly mutable loci in pathogenic bacteria. *Curr Biol.* 1994 4(1):24-33.
56. Bull JJ, Vegge CS, Schmerer M, Chaudhry WN, Levin BR. Phenotypic resistance and the dynamics of bacterial escape from phage control. *Plos One.* 2014;9(4):e94690.
57. Cota I, Sanchez-Romero MA, Hernandez SB, Pucciarelli MG, Garcia-del Portillo F, Casades J. Epigenetic Control of *Salmonella enterica* O-Antigen Chain Length: A Tradeoff between Virulence and Bacteriophage Resistance. *Plos Genetics.* 2015;11(11):e1005667.
58. Ongena V, Mabrouk AS, Crooijmans M, Rozen D, Briegel A, Claessen D. Reversible bacteriophage resistance by shedding the bacterial cell wall. *Open Biology.* 2022;12(6):210379.
59. Wohlfarth JC, Feldmüller M, Schneller A, Kilcher S, Burkolter M, Meile S, et al. L-form conversion in Gram-positive bacteria enables escape from phage infection. *Nature Microbiology.* 2023.
60. Meaden S, Paszkiewicz K, Koskella B. The cost of phage resistance in a plant pathogenic bacterium is context-dependent. *Evolution.* 2015;69(5):1321-8.
61. Hernandez CA, Koskella B. Phage resistance evolution *in vitro* is not reflective of *in vivo* outcome in a plant-bacteria-phage system. *Evolution.* 2019;73:2461-75.
62. Eriksen RS, Svenningsen SL, Sneppen K, Mitarai N. A growing microcolony can survive and support persistent propagation of virulent phages. *Proc Natl Acad Sci USA.* 2018;115(2):337-42.
63. Schrag SJ, Mittler JE. Host-parasite coexistence: The role of spatial refuges in stabilizing bacteria-phage interactions. *Am Nat.* 1996;148(2):348-77.
64. Simmons EL, Bond MC, Koskella B, Drescher K, Bucci V, Nadell CD. Biofilm Structure Promotes Coexistence of Phage-Resistant and Phage-Susceptible Bacteria. *mSystems.* 2020;5(3):e00877-19.
65. Testa S, Berger S, Piccardi P, Oechslein F, Resch G, Mitri S. Spatial structure affects phage efficacy in infecting dual-strain biofilms of *Pseudomonas aeruginosa*. *Commun Biol.* 2019;2:405.
66. Attrill EL, Claydon R, Łapińska U, M. R, Meaden S, Brown AT, et al. Individual bacteria in structured environments rely on phenotypic resistance to phage. *PLoS Biol.* 2021;19(10):e3001406.
67. Brockhurst MA, Buckling A, Rainey PB. Spatial heterogeneity and the stability of host-parasite coexistence. *J Evol Biol.* 2006;19(2):374-9.
68. Fiegna F, Velicer GJ. Exploitative and hierarchical antagonism in a cooperative bacterium. *Plos Biol.* 2005;3(11):1980-7.
69. Pitcher DG, Saunders NA, Owen RJ. Rapid Extraction of Bacterial Genomic DNA with Guanidium Thiocyanate. *Lett Appl Microbiol.* 1989;8(4):151-6.
70. Domenico P, Schwartz S, Cunha BA. Reduction of capsular polysaccharide production in *Klebsiella pneumoniae* by sodium salicylate. *Infect Immun.* 1989;57(12):3778-82.
71. Blumenkrantz N, Asboe-Hansen G. New method for quantitative determination of uronic acids. *Anal Biochem.* 1973;54(2):484-9.
72. Steinegger M, Soding J. MMseqs2 enables sensitive protein sequence searching for the analysis of massive data sets. *Nat Biotechnol.* 2017;35(11):1026-8.
73. Seemann T. Prokka: rapid prokaryotic genome annotation. *Bioinformatics.* 2014;30(14):2068-9.

74. Graziotin AL, Koonin EV, Kristensen DM. Prokaryotic Virus Orthologous Groups (pVOGs): a resource for comparative genomics and protein family annotation. *Nucleic Acids Res.* 2017;45(D1):D491-D8.
75. Eddy SR. Accelerated Profile HMM Searches. *PLoS Comput Biol.* 2011;7(10):e1002195.
76. Arndt D, Grant JR, Marcu A, Sajed T, Pon A, Liang Y, et al. PHASTER: a better, faster version of the PHAST phage search tool. *Nucleic Acids Res.* 2016;44(W1):W16-21.
77. Rendueles O de Sousa JAM, Rocha EPC. Competition between lysogenic and sensitive bacteria is determined by the fitness costs of the different emerging phage-resistance strategies| 2023 | doi: 10.6084/m9.figshare.22101998

ACKNOWLEDGEMENTS

The sequencing work was made at the Biomix Platform, C2RT, Institut Pasteur, Paris, France, supported by France Génomique (ANR-10-INBS-09) and IBISA. We thank Alex Hall for critical reading of the manuscript. We would also like to thank the reviewers for their contribution which critically improved the manuscript.

FUNDING

This work was funded by an ANR JCJC (Agence national de recherche) grant [ANR 18 CE12 0001 01 ENCAPSULATION] awarded to O.R. The laboratory is funded by a Laboratoire d'Excellence 'Integrative Biology of Emerging Infectious Diseases' (grant ANR-10-LABX-62-IBEID) and the FRM [EQU201903007835]. The funders had no role in study design, data collection and interpretation, or the decision to submit the work for publication.

COMPETING INTERESTS

Authors declare that we do not have any competing interests in relation to the work described.

DATA AVAILABILITY

All raw data is available on figshare.com; 10.6084/m9.figshare.22101998 (77)

FIGURE LEGENDS

Figure 1. Fitness of strains during competition. **A.** The competitive index is calculated as the final frequency of each strain divided by the initial frequency in the mixed cocultures. * $P < 0.05$, Wilcoxon rank sum test adjusted by Benjamini-Hochberg correction. **B.** The effect of mixing two strains during growth in coculture is given as $Ci(j)$, expressed in \log_{10} , with i representing either strain BJ1 or strain ST14. Positive values represent increased cell numbers during coculture than those expected from the pure cultures. P values corresponds to one-sample t-test for difference of 0. * $P < 0.05$, *** $P < 0.001$. Each dot shape represents an independent experiment, $N=5$. Error bars indicate the standard deviation.

Figure 2. Coevolution of the two strains during 30 days. **A.** Total CFU per mL of each strain as estimated every day on selective media. Each line represents an independent coevolving population. **B.** Emergence of non-capsulated mutants in each strain. The proportion of capsulated clones in the population is depicted. The insert shows the area under the curve (AUC) during the first 9 days of evolution, as calculated by the function *trapz* from the R package *pracma*. * $P < 0.05$, ** $P < 0.01$, *** $P < 0.001$ for ANOVA with Tukey *post hoc* corrections.

Figure 3. Evolution of resistance mechanisms in strain BJ1. **A.** Ratio of clones from each coevolving population that are susceptible (green), non-capsulated (light pink), capsulated lysogens (beige), or capsulated but resistant by other undefined mechanisms (dark pink). N.B. Dashed line indicates when x-axis, no longer follows a linear scale. Dark arrows indicate lysogens tested in panel C. **B.** Growth of newly lysogenized clones reveal significant death during exponential phase (in the absence of induction), as measured by the optical density. Black line corresponds to the control, BJ1 ancestor. All independent growth curves, with and without induction are represented in Figure 3 – Figure Supplement 1. **C.** PFU/mL produced without induction by five selected new lysogens derived from BJ1 and isolated at day 1 for A4 and A6 (Population #2, MMC), at day 4 for B3 (Population #3, MMC) and day 9 for H8 and H9 (Population #3, MMC). Dashed line indicates the limit of detection of the essay. Each black dot represents an independent biological replicate (independent strain lysate) and large red dots represent the mean. Error bars correspond to the standard deviation. Two-sided t-test ‘a’, $P < 0.001$ compared to ancestor BJ1 (negative control, C-) and ‘b’, $P < 0.05$ compared to ST14 (phage producer, positive control, C+). **D.** Simulated temporal dynamics of proportion

of lysogens in the populations, as calculated by eVIVALDI. Each circle corresponds to the central tendency of replicate simulations, with the different colours indicating a given probability of spontaneous prophage induction (shown in the legend, values approximated to nearest major integer). The error bars correspond to the standard deviation across the replicate simulations. In the represented simulations, the probability of acquisition of a phage resistance mutation (capsule loss) is 0.001, and the fitness cost of this mutation is 10% of the bacterial growth rate, as calculated in (43).

Figure 4. Growth of BJ1 resistant clones. All isolated clones that were capsulated and tested for resistance (Figure 3A and Figure 3 – Figure Supplement 1) were grown in the absence of phage (control) or with phage. One or two non-capsulated clones per day were randomly selected and included in the analyses. The area under the growth curve of each clone was estimated, and compared to that of the BJ1 ancestor (dashed line). K-W, Kruskal-Wallis test. *Post hoc* tests for significant differences across groups was calculated and p-values adjusted for multiple testing with Bonferroni correction. *a*, $P < 0.05$ difference from non-capsulated; *b*, $P < 0.05$ difference from resistant by other mechanisms; *c*, $P < 0.05$ difference from lysogens; *d*, $P < 0.05$ difference from sensitive strains.

Figure 5. Characteristics of phage resistant clones. **A.** Schematic organization of the capsule operon of strain BJ1. Black triangles represent mutations observed in the capsule operon. Blue arrows indicate core genes common to all *K. pneumoniae* capsule serotypes. Grey arrows correspond to serotype-specific genes. GT stands for glycosyltransferase. The diagram was generated with genoplots package. **B.** For each clone, we evaluated the amount of capsule produced, the ability of the phage to be adsorbed and phage the sensitivity on overlay by EOP (PFU/mL) and on liquid culture by AUC. The AUC difference accounts for the surplus of growth of the control compared to growth with phage. If the clone is resistant, the difference in AUC is ~ 0 . The average of three independent replicates is shown. The experiments were performed with three independently generated lysates, when applicable. ND: none detected.

Figure 6. Transient resistance to phages. The difference in the area under the curve (AUC) represents the effect of adding phage to a growing culture as estimated by the difference in growth curve in the absence of phage and with phage (Figure 6 – Figure Supplement 1). Values below 0 indicate strains are sensitive to phage, and values close to 0 indicate that there

is no effect of adding phage to the culture. Non-conditioned clones are those directly grown from glycerol stock, whereas pre-conditioned clones, had been reisolated twice, and grown overnight prior to performing the growth analyses. The ancestor, BJ1, sensitive, and the non-capsulated mutant ($\Delta wcaJ$), are included as controls for the difference in culture conditions. Statistics represent t-tests to check from differences between clones directly from stock and those sequenced (after two passages in LB). ns means non-significative, * $P < 0.05$, ** $P < 0.01$ and *** $P < 0.001$.

Figure 7. Cross resistance to phages from other lysates. A. The area under the curve for capsulated (and non-lysogenized) resistant clones was calculated. The AUC of control cultures with LB was subtracted from those that were challenged with phage lysates. (Growth curves are shown in Figure 7 – Figure Supplement 1A). Each dot represents an independent assay. One-sample t-tests were performed to test the difference from 0 (growth in LB). * $P < 0.05$; ** $P < 0.01$ **B.** PFU/mL of three independently generated lysates on lawns of new BJ1 lysogens from different evolutionary treatments. Lysogens A4 and A6 evolved in MMC and were isolated at day 1, lysogens B5 and D111 evolved in LB and were isolated at day 6 and 7 respectively, and clone F5 evolved in citrate and was isolated at day 7. Each black dot represents an independent assay. The dashed line represents the limit of detection of the assay.

988

989 SUPPLEMENTARY MATERIAL LEGENDS

990

991 **Figure 1 – Figure Supplement 1. Growth and phage production in experimental**
992 **conditions.** **A.** Growth of each strain and their coculture in each experimental condition.
993 Three independent clones and cocultures were measured. **B.** Area under the growth curves,
994 calculated with *trapz* function from *pracma* package for R. **C.** Citrate amount in 24-hour
995 cultures of strain BJ1, ST14, 1:1 coculture and control cultures of plain LB with citrate. Each
996 dot represents an independent experiment. Error bars indicate standard deviation. **D.** Strain
997 ST14 was grown in LB, in LB diluted (1:1) in spent supernatant from BJ1, or in LB diluted
998 (1:1) in PBS. Phage lysates were prepared and PFU analysed on a lawn of strain BJ1. Each
999 dot represents an independent biological replicate. Error bars indicate standard deviation. **E.**
1000 Lysis plaques on an overlay of strain BJ1 after addition of 10 ul of supernatant of strain ST14
1001 grown in the different experimental conditions. * $P < 0.05$, ** $P < 0.01$, *** $P < 0.001$ for
1002 ANOVA with Tukey *post hoc* corrections.

1003

1004 **Figure 1 – Figure Supplement 2. Total growth in the different media.** **A.** The effect of
1005 mixing on total growth or population yield is expressed as $Bi(j)$, in which positive values
1006 represent more growth during coculture than expected from the pure cultures. Each shape
1007 represents an independent experiment, $N=5$. Error bars indicate standard deviation. **B.** The
1008 total yield of each culture is expressed as the \log_{10} -transformed of CFU/mL. Each shape
1009 represents an independent biological replicate, $N=5$. P-values correspond to Kruskal-
1010 Wallis(K-W) rank sum test, followed by pairwise Wilcoxon test for differences across
1011 conditions, with Benjamini-Hochberg correction. * $P < 0.05$

1012

1013 **Figure 2 – Figure Supplement 1. Total number of cells across evolving populations.** Each
1014 independent line represents an independently evolving population. Bold lines represent
1015 regression line from a linear model. The slopes of regression model were calculated for each
1016 independent population, and tested with a one-sample t-test for significant difference from 0.

1017

1018 **Figure 2 – Figure Supplement 2. Estimated phage titers in each population throughout**
1019 **the coevolution experiment.** Phages were estimated by plaque counting on ancestral phage
1020 susceptible BJ1. Total phage production was inferred for each population by quantifying the

efficiency of plaquing (EOP) of one capsulated and one non-capsulated randomly selected ST14 clone, relative to their presence in the population. Different shapes represent independently evolving populations.

Figure 3 – Figure Supplement 1. Number of clones from strain BJ1 analysed each day from each population. Each day a total of 93 capsulated clones from every population in each evolutionary treatment were isolated, except for day 1, when 186 capsulated clones (93 x 2) were isolated. The number of 93 was chosen for it to conveniently fit in a 96-well plate and allowing three wells for internal controls (ancestors and blank).

Figure 3 – Figure Supplement 2. Lysogens can release viable phages that infect the ancestral BJ1 strain. 93 lysogens were grown overnight in 100 µL of LB in a 96-well microtiter plate. Cultures were then diluted 1:100, and allowed to grow for 6 hours (A, non-induced lysogens), or two hours, after which, MMC was added to a final concentration of 5 µg/mL (B, induced lysogens). Cultures were allowed to grow for 4 more hours. After a total of 6 hours of overday growth, the microtiter plate was centrifuged to allow cells to pellet, and 4 µL of the supernatant was spotted on an overlay of 0.7% Lennox agar with the ancestral BJ1 strain. Two controls are included; ancestral BJ1(well H11) and ancestral ST14 (well H12).

Figure 3 – Figure Supplement 3. Growth of newly lysogenized clones. Clones were grown in either LB (control, grey line) for 16 hours or in LB to which MMC (1 µg/ml) was added after 1.5 hours (green). Labels on top of each graph correspond to the isolation day, population number, clone ID and condition in which it evolved. Star (*) indicates clones in which death is observed at the end of exponential phase, suggestive of unusually large phage outburst. Only one replicate per curve is shown for clarity purposes.

Figure 3 – Figure Supplement 4. Simulated temporal dynamics of the competition between different phage resistance mechanisms. eVIVALDI was used to simulate a scenario where an initial population of phage-sensitive bacteria ($n=\#$) is co-inoculated with $\#$ temperate phages. Upon infection, bacteria either die from the phage's lytic cycle or become lysogens if the phage follows the lysogenic cycle. Integrated phage (prophages) can subsequently spontaneously induce and restart the lytic cycle, leading to bacterial death. Bacteria can also become phage-resistant (before or after becoming lysogens) by random

mutation that represents the loss of the capsule. **A.** Heatmap of the proportion of lysogens in the populations at intermediate (t=10) and final (t=149) timepoints, as a function of the spontaneous induction probability (y-axis) and the probability of phage resistant (capsule-less) mutants to emerge. The fitness cost of the resistant mutants is fixed at 10%. **B.** Heatmap of the proportion of lysogens in the populations at intermediate (t=10) and final (t=149) timepoints, as a function of the spontaneous induction probability (y-axis) and the fitness cost of a phage resistant mutation (loss of capsule). The probability of these mutations to emerge is fixed at 0.001. For B, C and D, dark red colors indicate a prevalence of lysogens in the population, while deep blue colors indicate their absence. Each square in the heatmaps represents the median of the 20 independent replicate simulations for each combination of parameters.

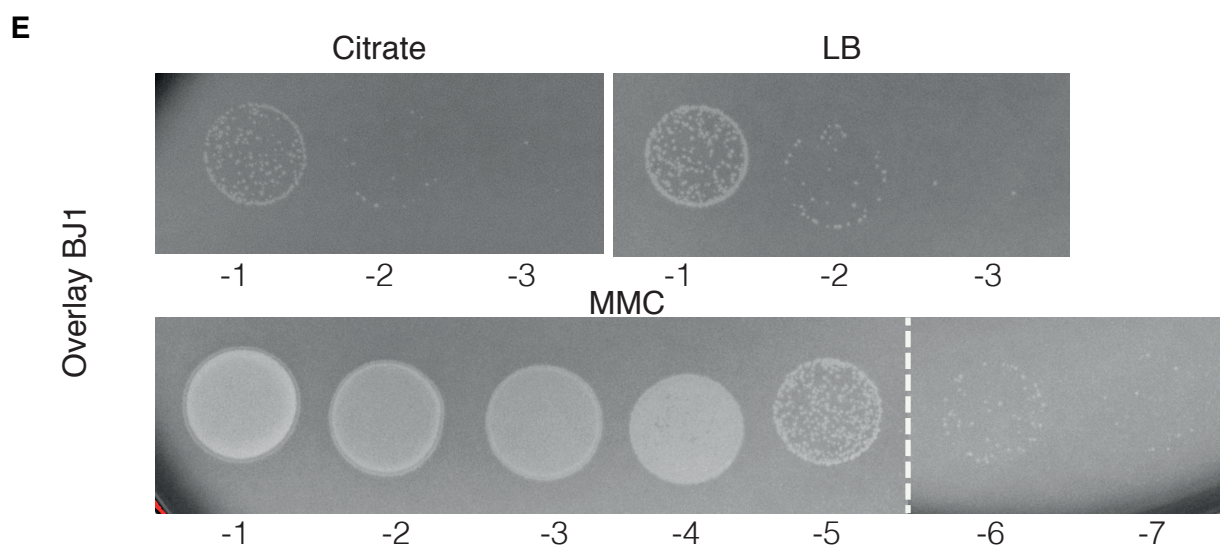
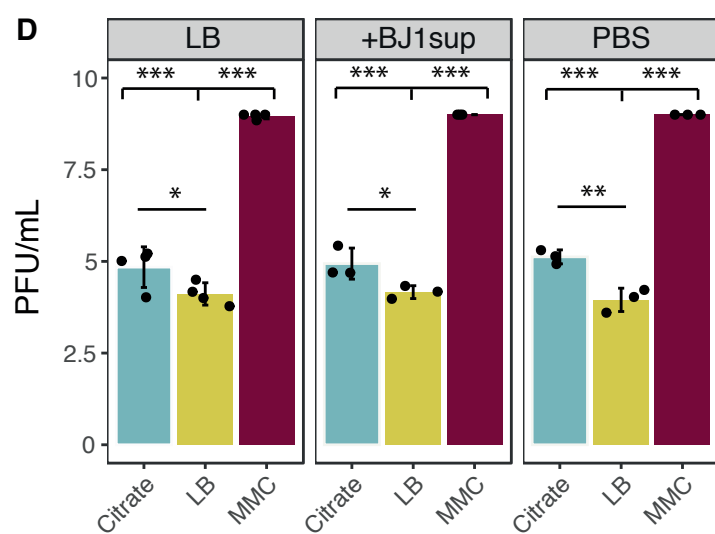
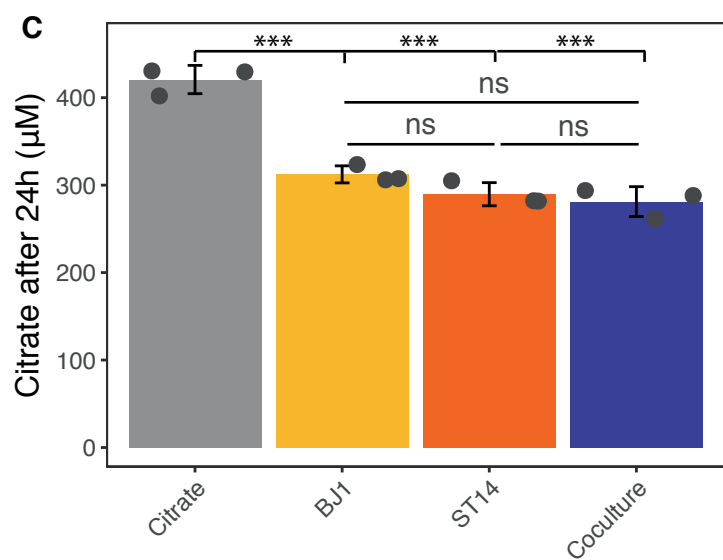
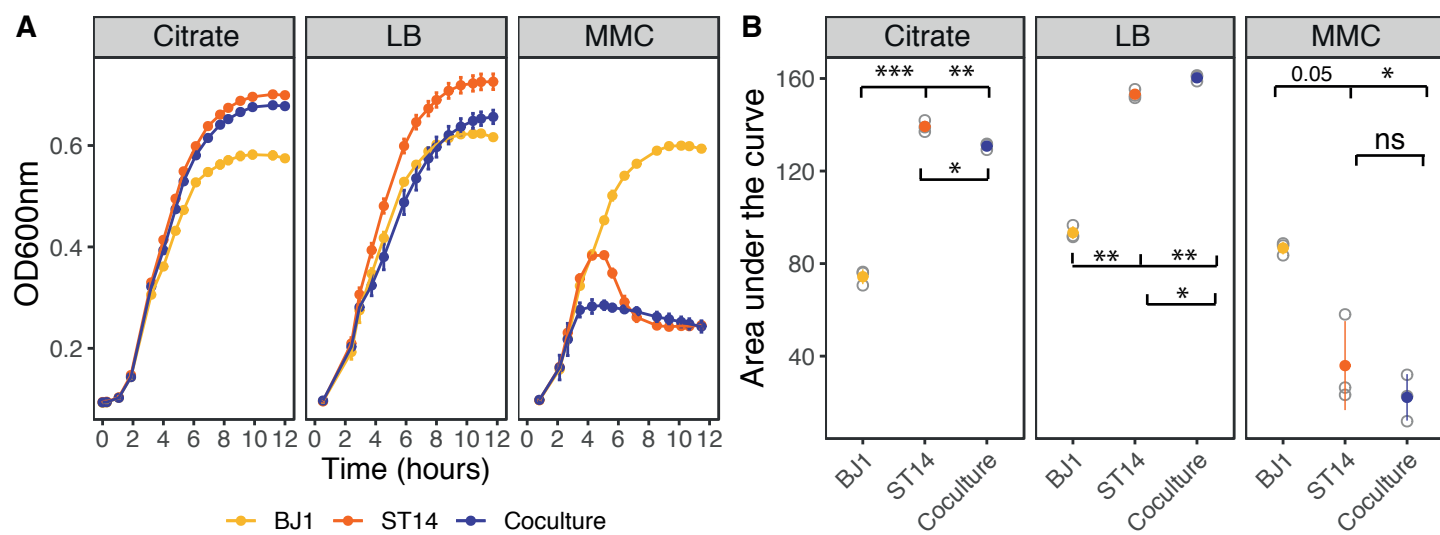
Figure 6 – Figure Supplement 1. Growth curves of resistant clones with no fixed mutations. Growth of resistant clones from the original stock were directly initiated from the glycerol stock without performing a preconditioning culture. Sequenced clones underwent two extra rounds of culture since the original stock; restreaked on agar and an overnight LB culture used to extract the genome and to generate a new glycerol stock, from which all other experiments were initiated. N=4. No error bars are shown for clarity purposes.

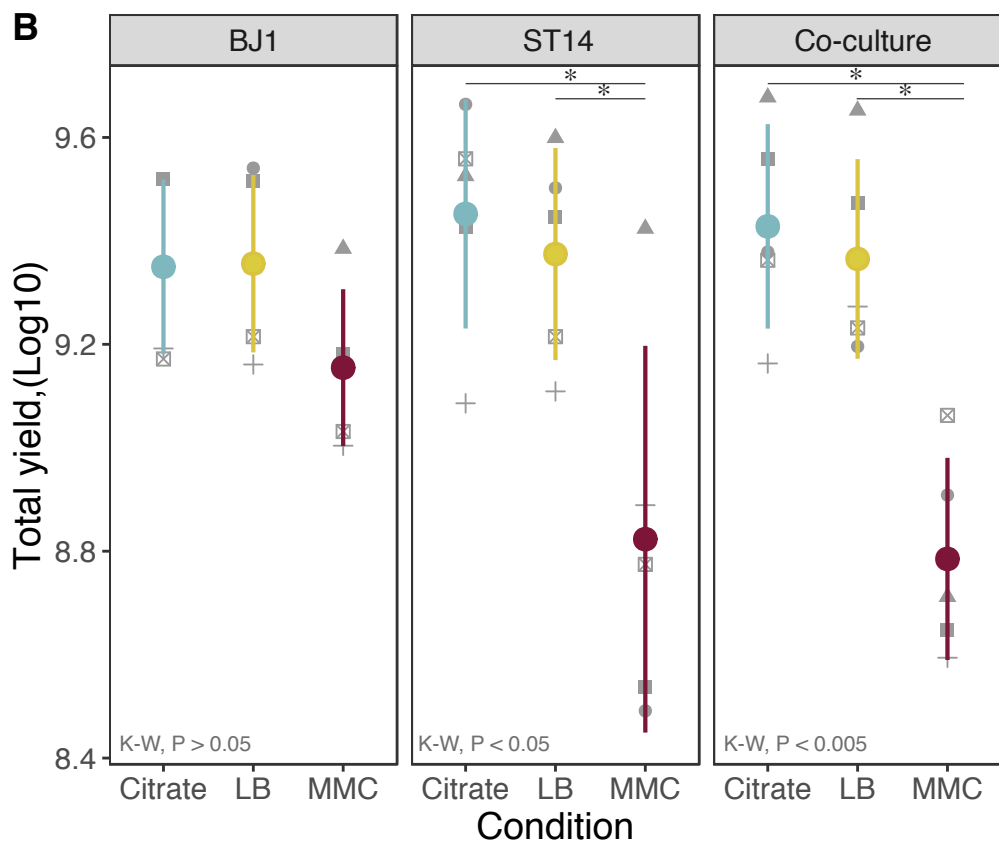
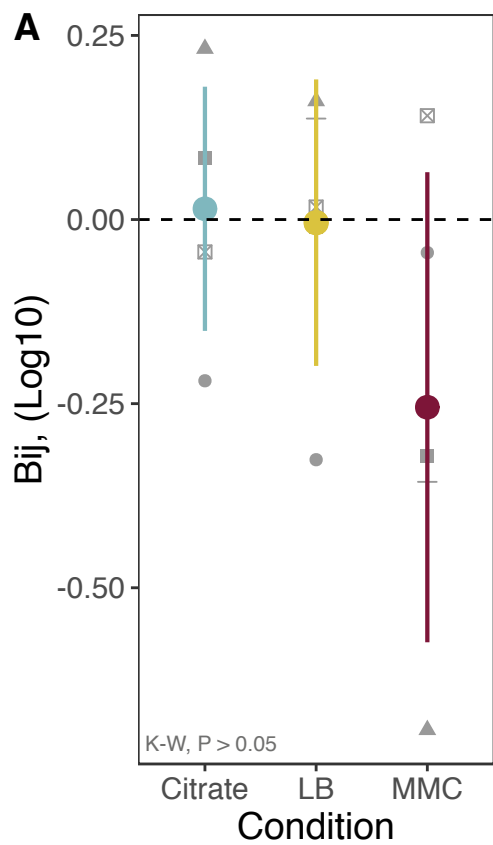
Figure 7 – Figure Supplement 1. Characterization of lysates produced by other K2 strains. **A.** Growth curves of resistant mutants and control strains in the presence of lysates produced by other K2 strains. Error bars are not shown to improve visibility. **B.** Phage similarity as expressed by wGRR of intact phages in lysates. **C.** Identity of proteins in intact phages present in other lysates against proteins in phages of strain ST14. (Only values > 0.5 as determined by BLASTP are displayed). **D.** Predicted function of proteins with an identity > 0.5. The functional characterization was performed by annotating the intact phages with prokka v1.14.0 (73), and pVOG profiles (74) searched for using HMMER v3.2 (75). For each protein, the pVOG with the lowest p-value was kept, and keywords analyzed.

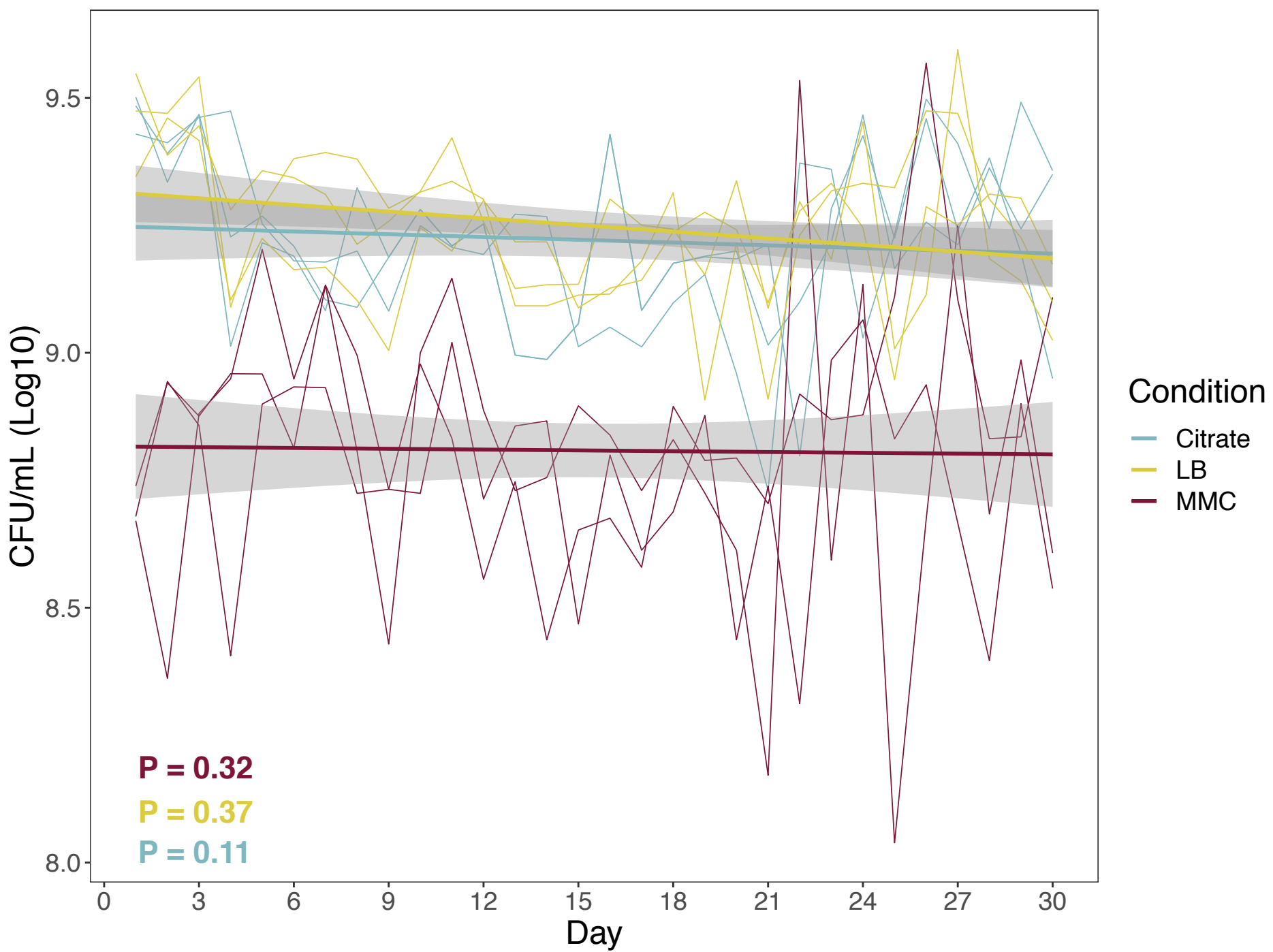
Supplementary File 1. PHASTER prophage prediction in strain ST14. The genome was analysed with PHASTER (76) in April 2021.

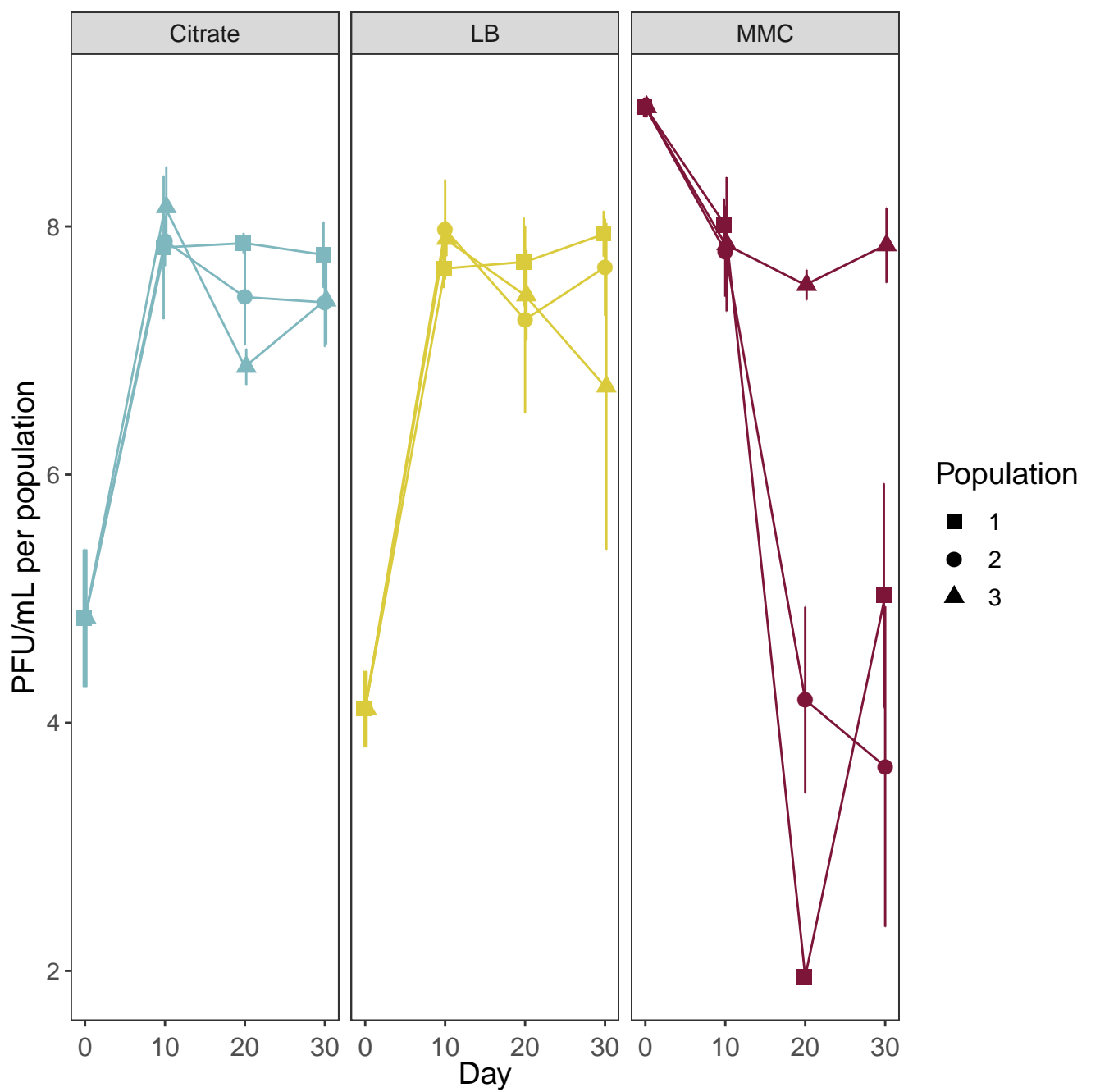
Supplementary File 2. Mutations accumulated in *wcaJ* gene resulting in non-capsulated mutants. ND; none detected. At the day in which at least 50% of the clones of each

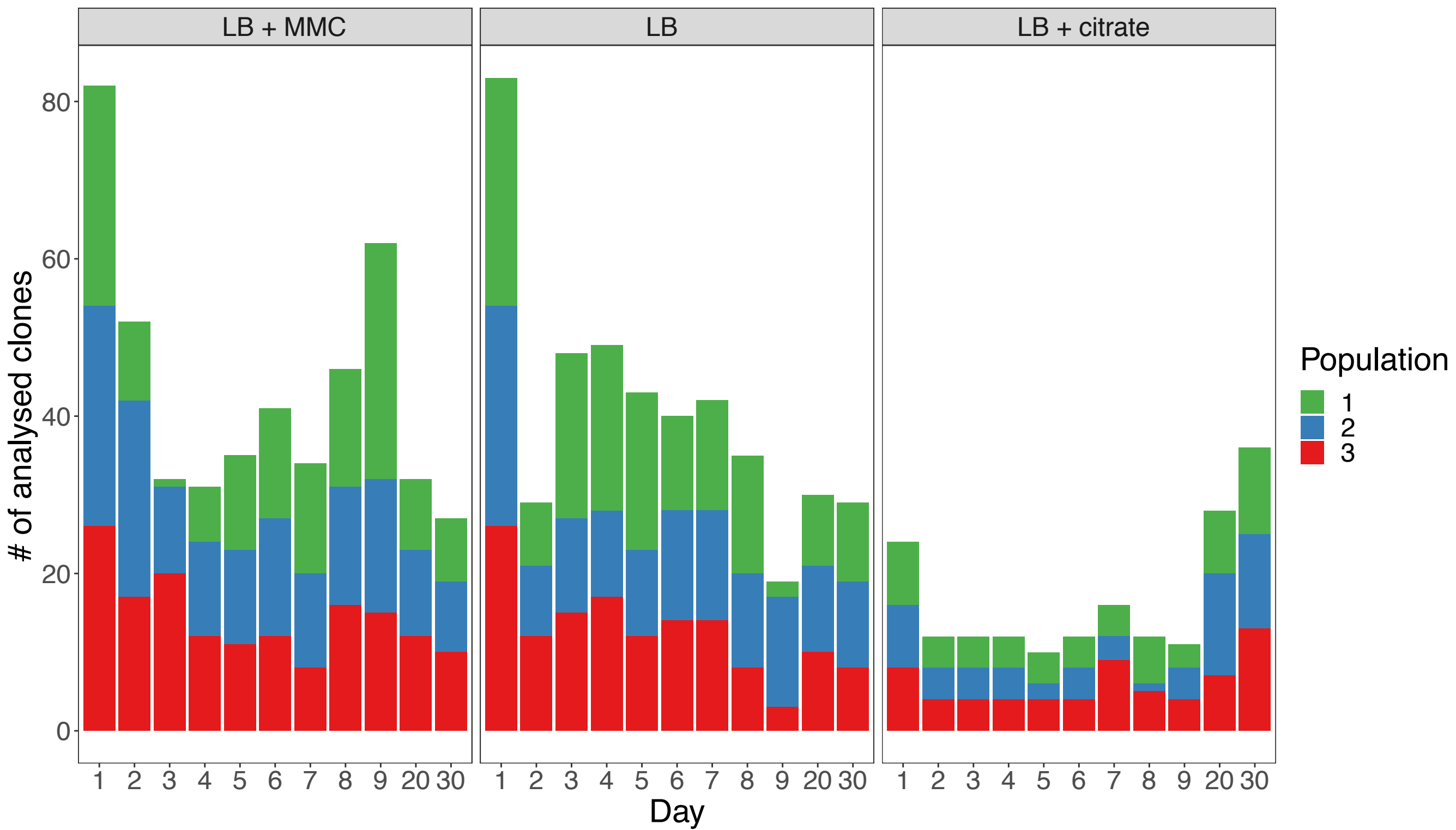
1089 independently evolving population were non-capsulated, two of such clones were isolated (#
1090 Clone), the *wcaJ* gene amplified by PCR and sequenced by Sanger. For BJ1, this was
1091 repeated twice independently (# Seq) (N=36 for BJ1 and N=18 for ST14). Independently
1092 evolving populations (Pop) are identified with number from 1 to 3. Sequencing of ancestor
1093 revealed that no mutations were present in the *wcaJ* genes.
1094

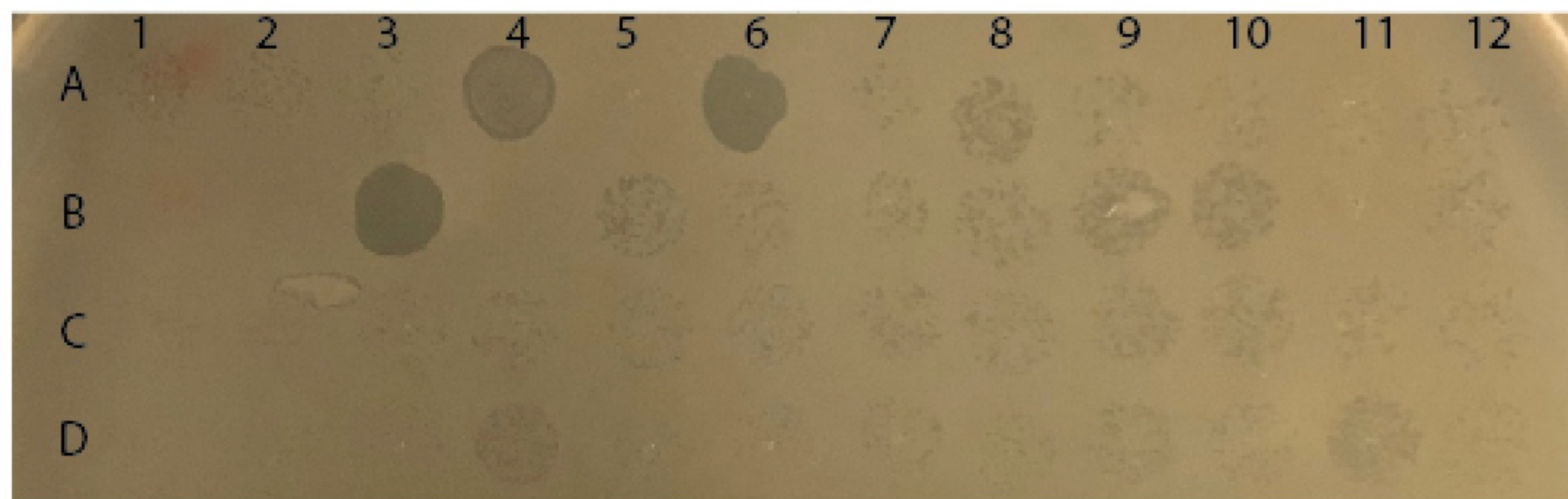
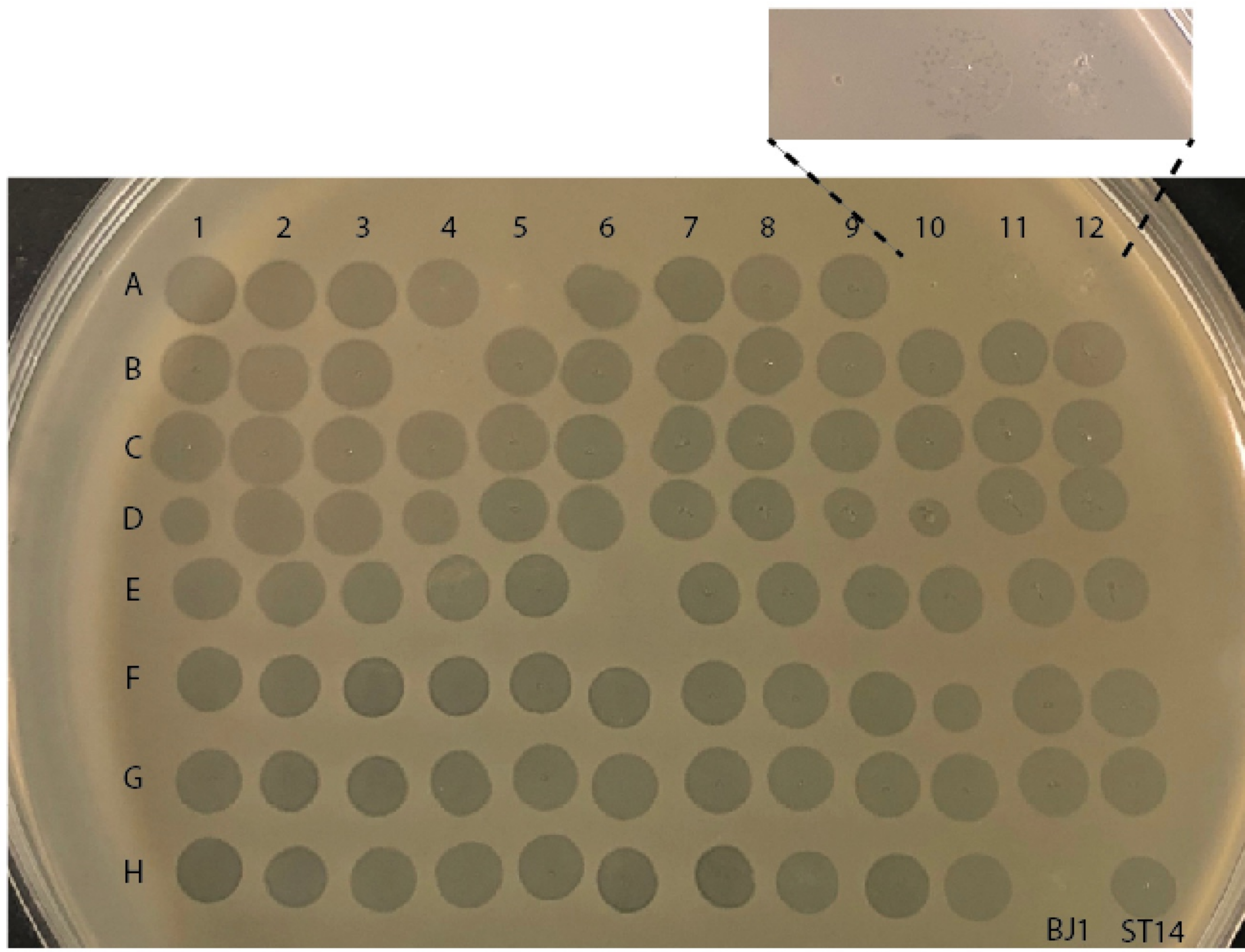




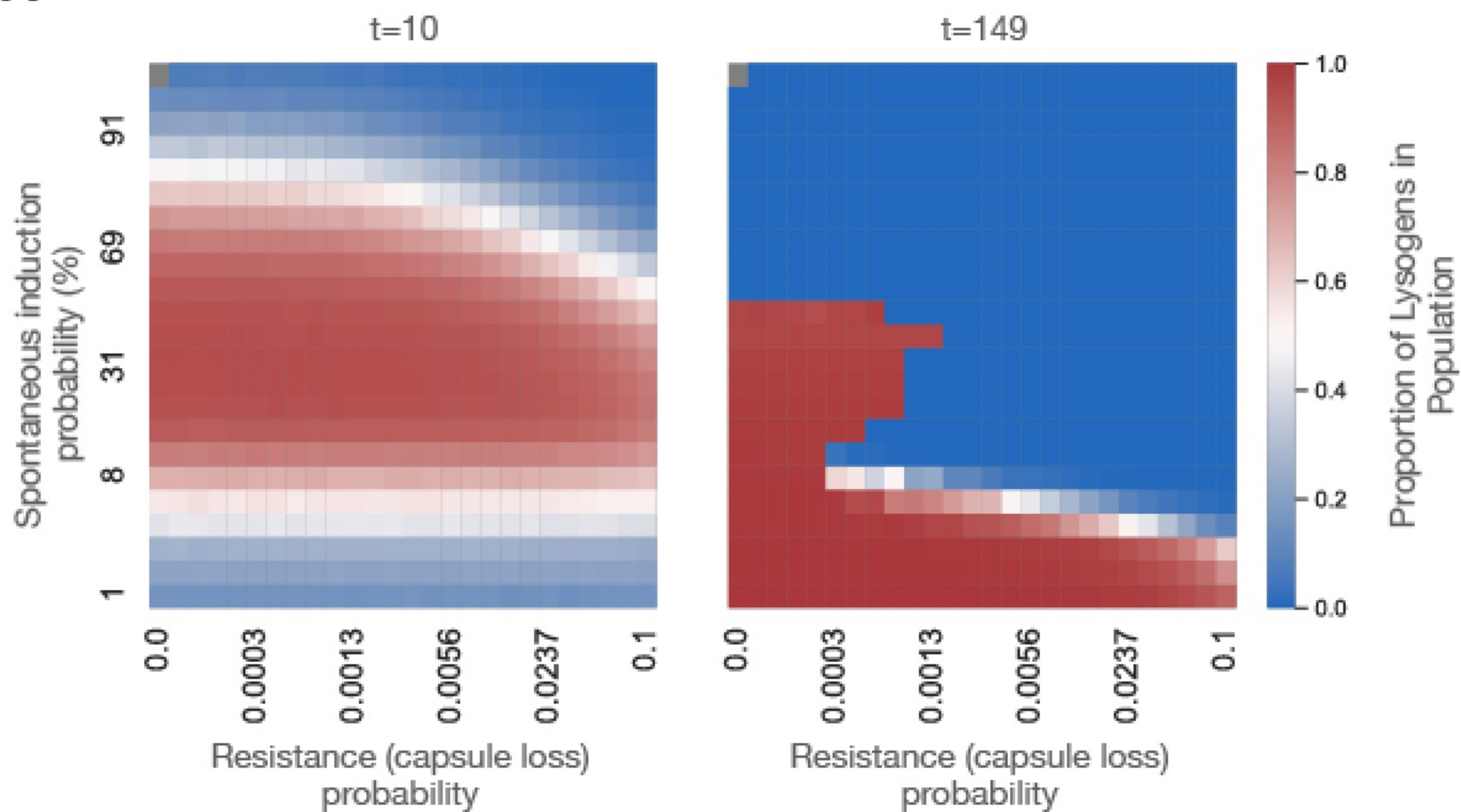
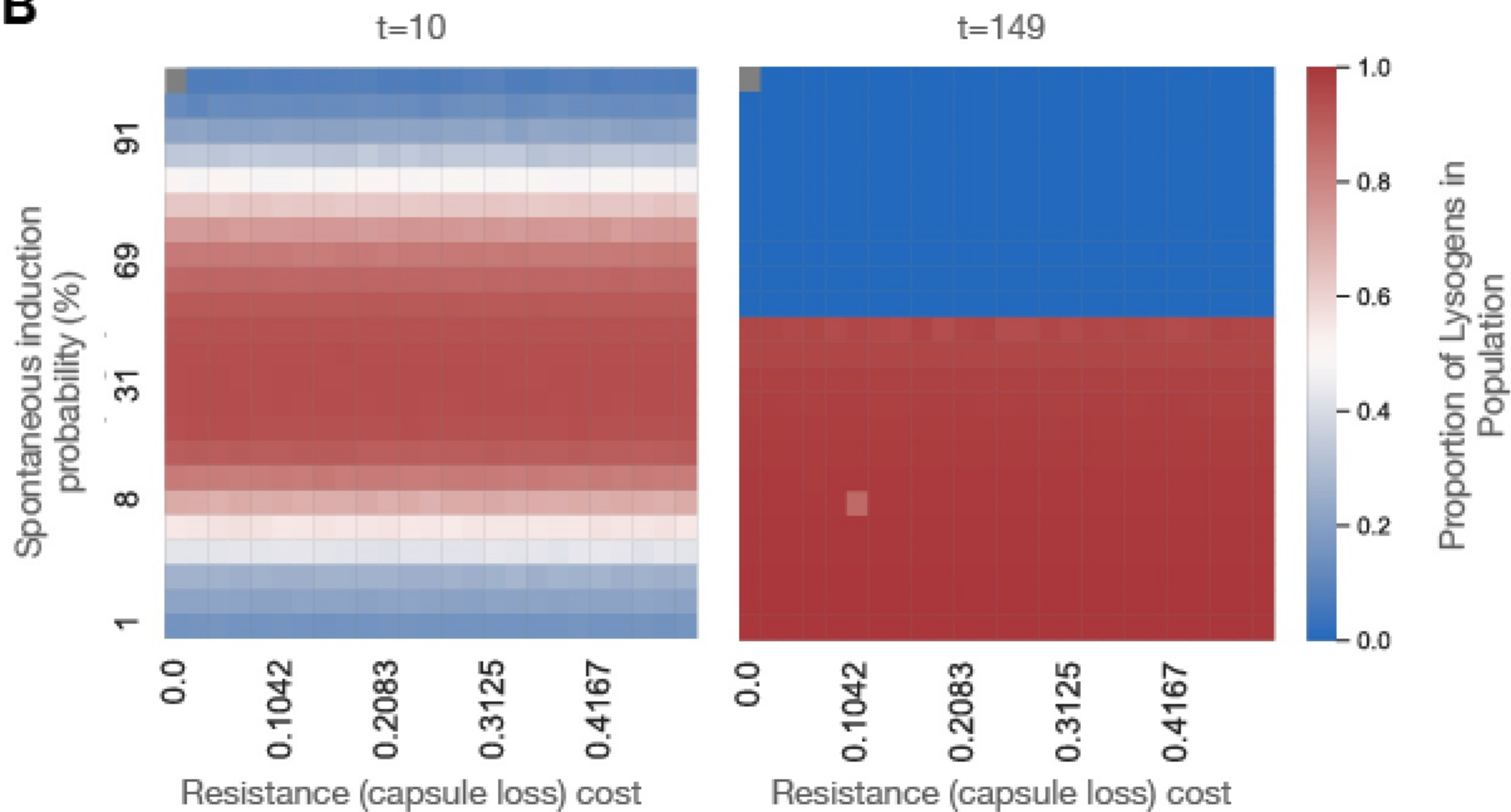


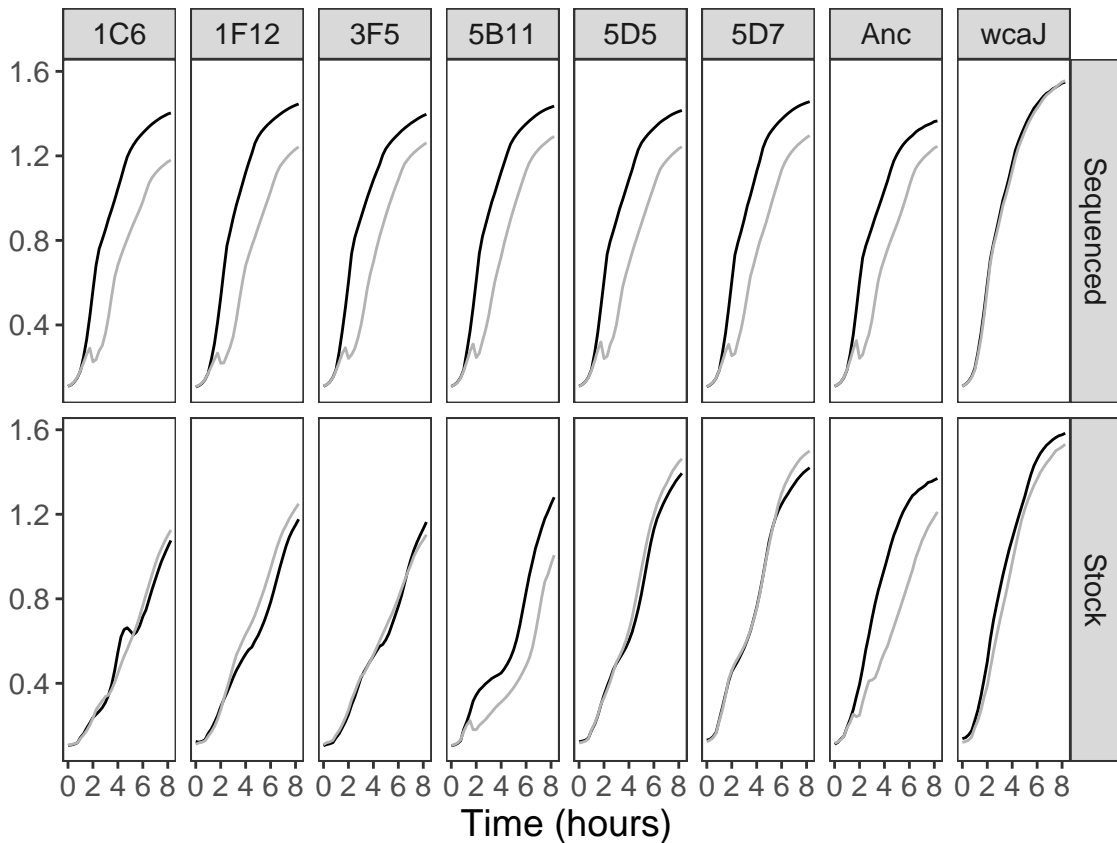




A**B**



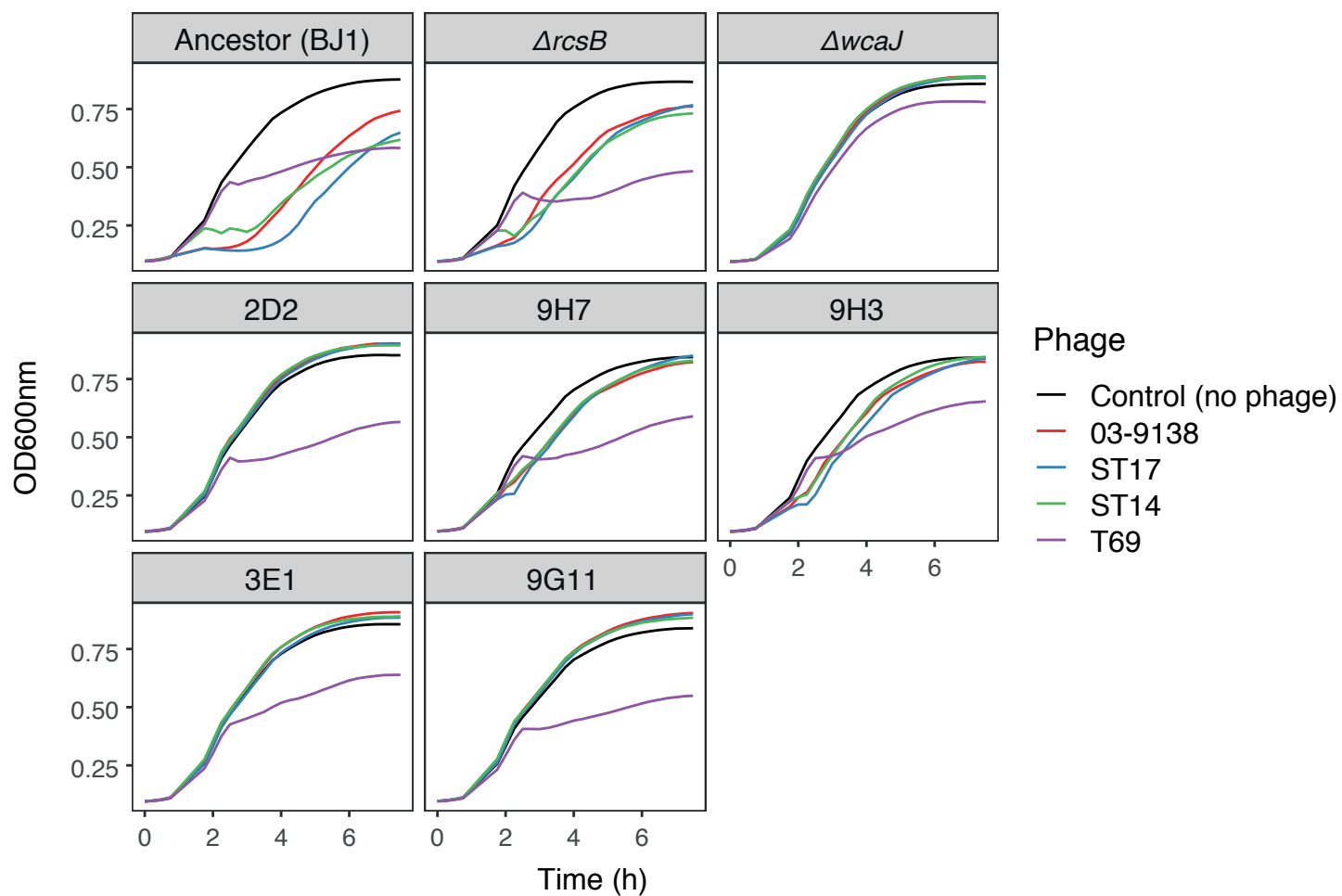
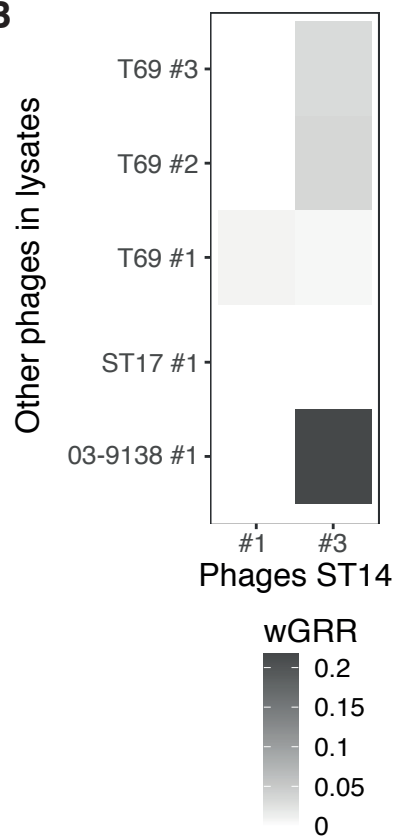
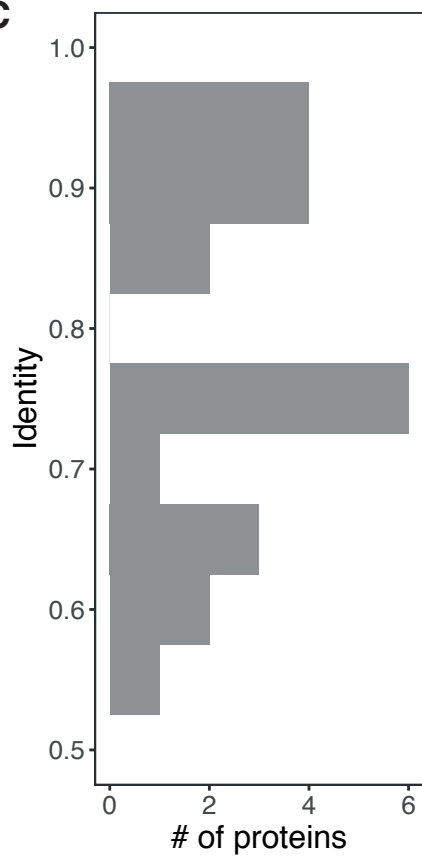
A**B**

OD_{600nm}

Condition

— LB

— Phage

A**B****C****D**